SULFUR ISOTOPE SEPARATION BY DISSOCIATIVE ELECTRON ATTACHMENT

By

JOHN EDWARD ALLEN, JR.

A DISSERTATION PRESENTED TO THE GRADUATE COUNCIL OF
THE UNIVERSITY OF FLORIDA
IN PARTIAL FULFILLMENT OF THE REQUIREMENTS FOR THE
DEGREE OF DOCTOR OF PHILOSOPHY

UNIVERSITY OF FLORIDA

1976

To

John and Michael

ACKNOWLEDGEMENTS

The author wishes to thank the members of his supervisory committee for serving in that capacity. In particular, deep appreciation is extended to his friend and advisor, Dr. Dennis R. Keefer, whose assistance and guidance were only exceeded by his patience. Sincerest gratitude is expressed to Dr. Willis B. Person for his interest and many inspiring discussions. He is also indebted to Dr. John R. Eyler for the use of and assistance with the ion cyclotron resonance apparatus. Thanks go to Dr. Robert L. Sierakowski and the Department of Engineering Sciences under the chairmanships of Dr. Knox Millsaps and Dr. Mark H. Clarkson for financial support.

It is with pleasure that he acknowledges Mr. J. D. McMillan and Mr. Jack VanLeer for making many pieces of equipment and for instructing the author in the fine art of machining. He also expresses his appreciation to Mr. Harry Stroud for procuring necessary materials on a moment's notice. Special thanks go to Mrs. Karen Ostrea for her excellent typing of the manuscript; her concern for its general appearance equaled the author's.

With the utmost gratitude the author thanks Dr. Jad Batteh and Dr. Harvey Schau for their encouragement and technical assistance, but foremost for their personal friendship. Finally, the author wishes to thank his family for their devotion and unwavering faith in his abilities.

TABLE OF CONTENTS

		Page
ACKNOWLEDGEMENTS		iii
LIST OF TABLES		vi
LIST OF FIGURES		vii
ABSTRACT		ix
CHAPTER		
I.	INTRODUCTION	1
II.	SULFUR HEXAFLUORIDE	11
	Infrared Spectrum	11
	Electron Attachment	17
	Potential Energy Diagram	27
III.	ELECTRON ATTACHMENT MECHANISM	35
IV.	EXPERIMENTAL EFFORTS	40
	Duplication of Reported Results	40
	Electron Gun Experiment	41
	Pulsed Hollow Cathode Experiments	44
V.	ION CYCLOTRON RESONANCE PROGRAM	48
	Kinetics Model	48
	Kinetics Model Predictions and Experimental Results	57
VI.	SUMMARY AND CONCLUSIONS	60

TABLE OF CONTENTS (Continued)

	Page
APPENDIX	62
THRESHOLD INTENSITY FOR LASER INDUCED ISOTOPE SEPARATION IN SULFUR HEXAFLUORIDE	62
Theoretical Considerations	63
Experimental Results	67
LIST OF REFERENCES	75
BIOGRAPHICAL SKETCH	79

LIST OF TABLES

Table		Page
1.	Fundamental vibrational frequencies for sulfur hexafluoride	14
2.	Isotope shifts for the ν_3 band of SF_6	18
3.	Parameters for the SF_6 and SF_6^- potential energy curves	29
4.	Reactions and rate symbols for the kinetics model	50
5.	Reaction rates for the kinetics program	54
A.1	Data for four threshold intensity experiments	73

LIST OF FIGURES

Figure		Page
1.	Structure of a sulfur hexafluoride molecule	12
2.	High-resolution spectrometer scan of the ν_3 band of SF_6	15
3.	Fine structure of the ν_3 band of SF_6 as obtained with a Pb_{1-x} Sn_x Se tunable semiconductor diode laser	16
4.	Kinetic diagram describing the reaction of SF_6 with electrons	19
5.	Internal energy distribution of neutral SF_6 at 300°K . .	22
6.	Temperature variation of the SF_5^- to SF_6^- ratio from 0 to 400°C. The solid line is taken from Reference 44 and the dotted line is an extrapolation of those data	24
7.	Potential energy curves for SF_6 and SF_6^-	31
8.	Experimental set up for separation of isotopes using the focused beam method	42
9.	Infrared spectra of SF_6. (a) Natural sample (b) Laser pulsed sample	43
10.	Infrared scans of SF_6. (a) Natural sample (b) Sample processed by the hollow cathode, then the laser (c) Sample processed by the laser, then the hollow cathode. .	47
11.	Production of SF_6^- and SF_5^- as determined by the kinetics program	55
12.	ICR trapped-ion spectrum for SF_6^- and SF_5^-	56
A.1	Two limiting cases for the reaction volume calculation	65

Figure		Page
A.2	Schematic diagram of the experimental set up	68
A.3	Infrared spectra of SF_6. (a) Before processing (b) After 100 pulses	71
A.4	Plot of $\ln (N_o/N)$ as a function of the number of laser pulses	72

Abstract of Dissertation Presented to the Graduate Council of the University of Florida in Partial Fulfillment of the Requirements for the Degree of Doctor of Philosophy

SULFUR ISOTOPE SEPARATION BY DISSOCIATIVE ELECTRON ATTACHMENT

By

John Edward Allen, Jr.

June, 1976

Chairman: Dennis R. Keefer
Major Department: Engineering Sciences

A new method is proposed for isotope separation in polyatomic molecules. In this method a laser is tuned to selectively excite a vibration mode of the molecules which contain the isotope to be removed. Before deactivation can occur, an electron is attached, resulting in an excited negative ion. Under the proper conditions this ion may dissociate, producing fragments which can be removed chemically. The initial isotopic mixture is depleted of this isotope and correspondingly enriched in other isotopes.

This technique is particularly suited to isotope separation in sulfur hexafluoride. Potential energy curves are developed for this molecule to aid in explaining the mechanism of dissociative electron attachment. These curves incorporate much of the information known about attachment of electrons to sulfur hexafluoride and represent an improvement over previously published curves. A rough estimate of the

effectiveness of this method is made, based upon the temperature-dependent branching ratio for SF_5^- and SF_6^-. The calculations indicate that the fractional ^{34}S content in a sample of processed sulfur hexafluoride may increase 4760 times the content in a natural sample.

A kinetics model is presented to describe the attachment of electrons to sulfur hexafluoride. Numerical solutions of the appropriate rate equations indicate that application of the proposed technique to sulfur hexafluoride will require a low pressure environment and a large number of zero energy electrons.

A simple theory is developed to determine threshold intensities for laser-induced dissociation on the basis of experimentally measurable quantities, the total laser power and the reaction volume. Using the focused beam method, a series of experiments performed to separate isotopes in sulfur hexafluoride establishes a value of 6.0 MW/cm^2 for the threshold intensity. This eliminates dissociative electron attachment as an explanation of isotope separation by the focused beam method, but does not exclude it as a viable technique for separating isotopes.

CHAPTER I

INTRODUCTION

Since its suggestion in the classic article by Schawlow and Townes[1] and initial development by Maiman,[2] the laser (Light Amplification by Stimulated Emission of Radiation) has rapidly moved from the realm of scientific curiosity to its present position as a useful tool. Today the laser can be found not only in the scientific laboratory, where its monochromaticity and coherence are allowing investigation of previously inaccessible areas, but also in such diverse places as the factory--where it is being used for welding automobile chassis and cutting and trimming transistors, the doctor's office--where treatment of glaucoma, retina attachment, and removal of polyps from vocal cords are being performed painlessly, and the planetarium--where the simulated night sky is being splashed with color by a dazzling laser light show. These are but a few in a long list of applications, a list that is growing daily as man's imagination finds new uses for this marvelous tool.

Two significant events in laser technology were the development of the helium-neon laser by Javan et al.[3] and the transversely excited atmospheric pressure (TEA) CO_2 laser by Beaulieu.[4] It had been felt that the most suitable lasing materials would be optically or electrically excited gases; however, prior to the development of the helium-neon laser,

lasing had only been achieved in solids, specifically ruby crystals. The disclosure of the helium-neon laser confirmed that gases could be made to lase and was the forerunner of the many gas lasers which are the mainstay of today's laser science and technology. Previous to the announcement of the TEA laser, operation of gas lasers was confined to pressures below atmospheric, severely restricting their output power by limiting the amount of lasing material. The CO_2 TEA laser permits a significant amount of energy to be discharged in a short period of time, thereby making high powers attainable. Because of its power capabilities and its range of operation--tunable from 9.6 μm to 10.6 μm--the CO_2 laser and in particular the TEA CO_2 laser has become the workhorse of industry and research.

With energy demands increasing and fossil fuel resources diminishing, it has become necessary to seek alternate means of energy, primarily electrical energy, production. A number of suggestions have been made as to how this may be accomplished; these include a greater dependence on fission reactors and the development of fusion reactors. It is in the fission and fusion efforts that the laser may make its most significant contributions.

Around the turn of the decade civilian fusion research was treated "like an eccentric uncle who must be humored but not supported."[5] Today, however, fusion is being touted as the energy panacea; indeed, when finally perfected, it will provide a source of energy that could conceivably last until our sun expires. Originally, fusion research was limited to the magnetic confinement approach, and in fact this may eventually prove to be the most successful method. Nevertheless, with

the advent of large-sized, powerful CO_2 and neodymium glass lasers, fusion schemes utilizing these lasers to compress and fuse pellets have become fashionable, allowing this area of research to enjoy unprecedented expansion. Despite the rapid growth and tremendous promise of this means of energy production, it is necessary to recognize that this is a long-term solution. Even the most optimistic workers in the field do not expect scientific breakeven for at least three years and an economical power source before the turn of the century.

In the short term, laser technology's most important contribution to the energy supply will likely be in enriching uranium to fuel light-water fission reactors and separating deuterium for use in heavy-water reactors. Currently, uranium is commercially enriched by taking advantage of the isotopic mass difference. Uranium in the form of gaseous uranium hexafluoride is processed through gaseous diffusion plants; the lighter isotope which diffuses more rapidly is thus separated. The major disadvantages to this method are the tremendous capital costs of a diffusion plant and the enormous amount of electrical energy needed for operation. Frequently quoted figures place the current cost of a diffusion plant at $3 billion and the power consumption of the three existing plants, when they are all operating at the same time, at 1.5% of the country's total electrical output.[6] Since enriched uranium fuel for the light-water reactor represents 5% of its capital cost, a savings would be realized from any technique that lowered the enrichment cost. A more significant savings could be gained for the heavy-water reactor if a more efficient procedure could be found for separating deuterium. These reactors operate on natural, that is, unenriched uranium and are appealing because

they would stretch current uranium supplies perhaps 100 years. However, deuterium is responsible for 25% of a heavy-water reactor's capital cost,[7] making it financially unattractive. Any reduction in the deuterium cost could have a decisive effect on the deployment of these reactors.

It has been estimated that uranium enrichment plants based on laser technology could produce savings of from $40 to $100 billion by the year 2000.[8] A laser-enrichment plant could perform more isotope separation per stage than a diffusion plant, therefore requiring fewer stages. This would result in massive capital investment savings per plant. The most dramatic savings would be in power consumption, since it is predicted that a laser facility would require 85% to 90% less power than a diffusion plant.[9] Since the laser process is more efficient than the diffusion process, it is figured that 40% more of the available uranium would be obtained from the feed ore.[8] This has a twofold effect: reduction of uranium costs and stretching of present supplies. It should be mentioned that another method for uranium enrichment is under development. Known as the centrifuge process, it would be competitive with the laser method on a power consumption basis; however, because of its greater efficiency the laser technique would result in 10% to 20% savings over the centrifuge system. The centrifuge process notwithstanding, laser separation of uranium on a commercial scale is close enough to prompt Edward Teller to remark "Whoever wants to start a separation plant today should carefully consider whether it is worthwhile starting it by one of the older techniques."[6]

As mentioned previously, separation of deuterium for heavy-water reactors may prove to be the laser's most significant contribution to

the energy problem. Since it only acts on the isotope of interest, the laser has a distinct advantage over other techniques. This advantage is more important for hydrogen with a hydrogen to deuterium ratio of 5000 to 1 than for uranium with a 238 to 235 ratio of 140 to 1. Reduction of the deuterium cost which is presently $50 per pound would encourage use of these environmentally safer reactors.

Having cited some of the advantages of laser isotope separation, it is instructive to consider, in general, how this is accomplished. Isotopes of a given element differ in their nuclear mass, one isotope possessing more neutrons than the other. These mass differences can result in a shift of an atom's electronic energy levels or a molecule's vibrational and rotational energy levels and are manifested as line shifts in atomic or molecular absorption spectra. As a result, the laser's monochromaticity permits excitation of a single species in an isotopic mixture. The excited species is then removed by a chemical or physical process. The basic prerequisites for isotope separation by lasers can therefore be summarized as [10].

1. An absorption spectrum with a well-resolved isotope shift.

2. A laser sufficiently monochromatic and tunable to excite the absorption of one isotope and not the other.

3. A chemical or physical process which acts on excited molecules and separates them from unexcited ones, but without a need for inherent isotopic selectivity.

4. A set of photochemical rate constants and physical conditions such that energy transfer from a laser-excited species to an undesired species does not occur before separation.

Several schemes for isotope separation have been proposed and subsequently reduced to practice. Although each method is based on the laser's monochromaticity to excite the desired isotope, each is different in the laser's effect on and the procedure for recovery of the designated isotope. One of the earliest proposals was the photodeflection method which has recently been executed by Bernhardt et al.[11] for a beam of barium atoms. If an atomic beam of natural isotopic abundance is crossed perpendicularly by a laser beam which is tuned to an absorption line of one of the isotopes, it is possible for that isotope to acquire momentum in the laser's propagation direction by absorption and emission of photons. When the number of photons scattered is large enough that the selected atom's momentum is comparable to or exceeds the spread in the atomic beam's transverse momentum, then separation has been achieved and it only remains to collect the desired isotope.

The method which has received the most attention for possible commercial separation of uranium isotopes is selective two-step photo-ionization. Successful application of this technique to the separation of uranium atoms was first announced by Exxon Nuclear Co.[12] based on a process developed and patented by Levy and Janes of Jersey Nuclear-Avco Isotopes, Inc.[13] Using a similar procedure, separation was also attained by Tuccio et al.[14] In both experiments isotopically mixed neutral uranium atoms emerging from a uranium oven are collimated and the desired isotopic atoms excited by a laser operating at a predetermined wavelength. The excited atoms are then ionized by a second laser or an ultraviolet source. Employing electric or magnetic fields the ions are deflected and collected.

Photochemical enrichment has recently been achieved for chlorine by Lamotte et al.[15] and Liu et al.[16] and for boron by Rockwood and Rabideau[17] and Freund and Ritter.[18] In these methods the laser is tuned to an absorption line of the preferred isotope. Excitation reduces the activation energy of a chemical reaction between those isotopes and a scavenger and increases the corresponding reaction rate. The resulting reaction products are found to be enriched in the designated isotope.

Selective dissociation has been the basis for isotope separation in several different molecular species. By photopredissociating formaldehyde Young and Moore[19] were able to enrich deuterium. Separation by photopredissociation is dependent on the selective excitation of isotopic spectral lines in a region of weak predissociation. In this region lines are sharp enough to resolve various isotopic molecules; consequently, excitation of a single absorption line yields isotopically pure dissociation products. Using a variation of the selective two-step photoionization method mentioned earlier, Ambartzumian et al.[20] were able to separate nitrogen isotopes by selectively dissociating ammonia. A pulsed CO_2 laser was tuned to selectively excite the vibrational transition of one isotope. The molecules were simultaneously illuminated by an ultraviolet source at a frequency sufficient to dissociate only the vibrationally excited molecules. Mass analysis of nitrogen molecules, one of the resulting dissociation products, showed a greater than natural abundance in the specified isotope.

A very simple method which has generated considerable interest and controversy is multiple photon absorption or, alternately, resonant infrared dissociation. This technique was first experimentally demonstrated

for boron trichloride by Ambartzumian et al.[21] Later the scheme was applied to sulfur hexafluoride by Ambartzumian et al.[22] and immediately thereafter, by Lyman et al.[23] To show that sulfur hexafluoride and boron trichloride are not unique in their isotopically selective multiple photon absorption and to establish a data base for theoretical development, Lyman and Rockwood[24] extended the method to difluorodichloromethane and silicon tetrafluoride. Each of the molecules mentioned have strong absorption features with measurable isotope shifts in either the 9.6 μm or 10.6 μm emission band of CO_2. To perform separation a CO_2 TEA laser is tuned to the absorption line of the isotope to be removed and the beam is focused in a low pressure cell containing the gas in its natural isotopic abundance. After pulsing the laser, analysis of the remaining gas shows a marked depletion of the designated isotope. The mechanism which leads to enrichment is not presently understood very well.

Previously, the economic advantages of a laser separation system over other systems were extolled. It seems appropriate at this point to consider the relative merits of the various laser schemes discussed above. To be commercially attractive, any proposed technique must be extendable to bulk processing. This eliminates the photodeflection method and to some extent selective two-step photoionization of atoms. An additional drawback to separation of atomic uranium is the difficulty of working with uranium vapor; it is very corrosive. For these reasons attention has centered on those methods which are applicable to separation of uranium isotopes in uranium hexafluoride. Since the largest isotope shift for uranium hexafluoride occurs at 16 μm, a true comparison of the

other schemes will await development of a laser emitting in this region, currently an area of active research.[25] However, on the basis of current knowledge about separation in other molecules, it is possible to draw some conclusions about these other techniques which can aid in guiding the research on uranium. The photochemical separation method has so far resulted in low enrichment yields. Of the remaining schemes multiple photon absorption requires the use of high power lasers and it is apparent that the 16 μm lasers under consideration will not be capable of delivering the required power. This leaves selective two-step photo-ionization of molecules as the technique being pursued most vigorously.

As an alternate explanation to multiple photon absorption for isotope separation of sulfur hexafluoride, Allen et al.[26] proposed the dissociative electron attachment mechanism. Based on recent studies of the visible luminescence associated with isotope separation in a focused beam,[27-30] it would appear that this is not the primary mechanism in operation. However, isotope separation by this method is appealing as evidenced by a recent presentation by Chen and Chantry[31] of Westinghouse Research Labs. The advantages of this method are that it would require only one laser which would not need to be high power and it would be suitable to bulk processing. Extension to uranium hexafluoride may be possible since, like sulfur hexafluoride, it has a high electron affinity. A detailed discussion of this scheme will be presented in the next chapter.

The underlying theme to the discussion so far has been the separation of isotopes for energy use and in particular uranium isotope separation. It would be logical to ask why enrichment of sulfur should

be of any interest. There are several reasons for this, one of which is sulfur hexafluoride's similarities to uranium hexafluoride, as was alluded to earlier. Not only do they both have high electron affinities, but also their general molecular structures are alike. Hence, many of the studies performed for sulfur may carry over to uranium. Probably the most significant reason is that the vibration of sulfur against the fluorine cage occurs "in a region where any good vibration should lie, namely in the carbon dioxide region."[32] This facilitates isotope separation experiments for sulfur. Comparable experiments for uranium must await the development of the proper laser, since in uranium hexafluoride this vibration lies at 16 μm as mentioned previously. Finally, enrichment of light isotopes in and of itself promises to be both important and profitable. For example, current costs per mole for enriched light isotopes range from $290,000 for sulfur 34 to $177 for boron 10.[33] Included in that range are the potentially important isotopes carbon 13, chlorine 37, nitrogen 15, and oxygen 18. These light isotopes may find application in the medical field, environmental research, or pollution detection. Indeed, if these isotopes are accessible and inexpensive, the list will grow as man finds new uses for them just as he has done for the laser.

CHAPTER II

SULFUR HEXAFLUORIDE

Sulfur hexafluoride is very efficient at capturing low energy electrons and considerable effort has been made to understand its electron attachment properties. This unusual feature makes SF_6 useful in the laboratory as an energy calibration for low energy electrons, a detector of scattered electrons, a scavenger or inhibitor in radiolysis experiments and in the electrical industry as a gaseous dielectric. More recently, attention has turned to the spectral chararacteristics of SF_6, since it readily absorbs CO_2 laser radiation. So, in addition to its uses as an electron absorber, SF_6 is now being employed as a nonlinear absorber for the attenuation of laser radiation.

Infrared Spectrum

The structure of sulfur hexafluoride is highly symmetrical with the sulfur atom at the center of a regular octahedron whose corners are occupied by six fluorine atoms as indicated in Figure 1.[34] This configuration was first suggested by electron diffraction measurements and later confirmed by Raman and infrared investigations. As a result of its octahedral geometry, this molecule belongs to the O_h point group and exhibits six normal vibrations--three Raman-active fundamentals, two infrared-active fundamentals, and one inactive fundamental. The six fundamental vibrational frequencies as measured by different

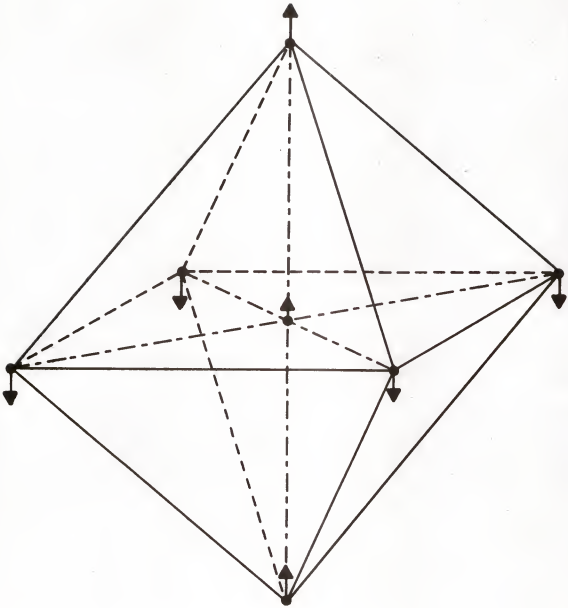

Figure 1. Structure of a sulfur hexafluoride molecule.

researchers[35,36] are listed in Table 1.

Current interest is centered on the ν_3 fundamental of SF_6 at 948 cm^{-1}, since this stretching mode contains vibration-rotation transitions that are nearly coincident with the CO_2 laser lines in the $00^01\text{-}10^00$ band at 10.6 μm. The nature of this vibration is indicated by the arrows in Figure 1; the sulfur and two fluorine atoms which lie along an axis of the octahedron move in one direction, while the other four fluorine atoms forming a plane travel in the opposite direction. To establish a reliable value for this frequency and to resolve the fine rotational structure of this band, which is necessary for identification of CO_2 laser pumped transitions, this vibration mode has been re-examined.[37-39] The spectrum of the ν_3 band, as recorded by a high-resolution infrared spectrometer, appears as Figure 2;[37] note that the rotational structure is not resolved. To illustrate the fine structure and to emphasize the diverse, dramatic applications of lasers, a portion of the same spectral region as recorded using a $Pb_{1-x}Sn_xSe$ tunable semiconductor diode laser is reproduced in Figure 3.[39] This latter measurement, which is extremely accurate, places the band center at 947.988 cm^{-1}, in good agreement with the value of 947.9 cm^{-1} obtained in the former experiment. Additional spectra of this quality will facilitate identification of transitions which can be laser excited.

Fluorine occurs naturally in only one isotopic form--^{19}F; however, there are four isotopes of sulfur which are naturally occurring. Each sulfur isotope produces a characteristic shift in the spectrum of SF_6. Knowledge of this isotope shift is important to laser separation processes; since, if the spectra of the various isotopes are significantly

Table 1.

Fundamental vibrational frequencies for sulfur hexafluoride

Activity	Assignment	Symmetry	Frequency cm^{-1}	
			Lagemann and Jones[35]	Gaunt[36]
Raman	ν_1	A_{1g}	775	775
Raman	ν_2	E_g	644	644
Infrared	ν_3	F_{1u}	940	932
Infrared	ν_4	F_{1u}	615	613
Raman	ν_5	E_{2g}	524	524
Inactive	ν_6	F_{2u}	363	344

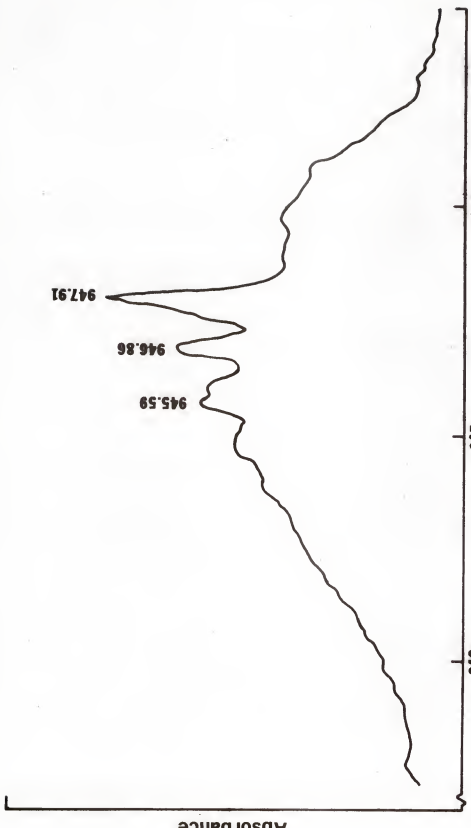

Figure 2. High-resolution spectrometer scan of the ν_3 band of SF_6.

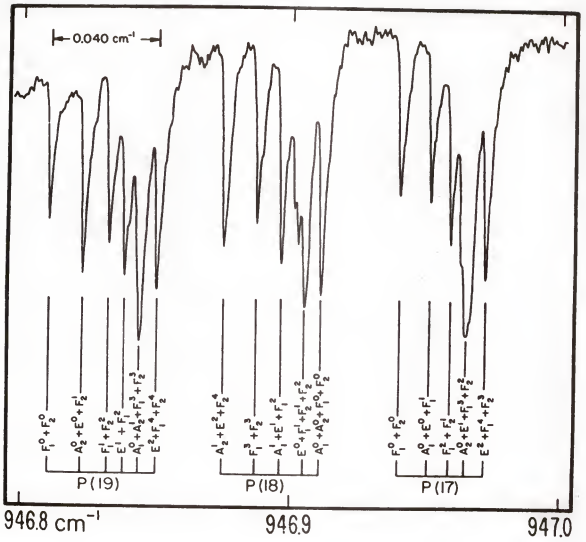

Figure 3. Fine structure of the ν_3 band of SF_6 as obtained with a $Pb_{1-x}Sn_xSe$ tunable semiconductor diode laser.

overlapped, selection of the desired isotope by a laser line becomes difficult. For SF_6 it has been found that the minimum isotope shift of the ν_3 band is 8 cm^{-1}[38] which is considerably larger than the line width of a CO_2 laser. Measured values for the isotope shifts of the SF_6 ν_3 band[37,38] and the natural abundance of the sulfur isotopes[40] are listed in Table 2.

Electron Attachment

Electron attachment to sulfur hexafluoride exhibits a number of interesting features which can best be described by referring to the simple kinetic diagram in Figure 4, which is similar to the one in Reference 41. As indicated, an SF_6 molecule can attach an electron possessing some kinetic energy E_{kin} with a rate k_f. This results in a negative ion complex which contains internal excitation at least equal to the electron affinity of the molecule. Subsequently, the complex may autodetach an electron (k_a), decompose to either SF_5^- and F (k_d) or $SF_5 + F^-$ (k_b), or be stabilized by collision with a species M($k_s[M]$), with the wall (k_w), or by a radiative process (k_r).

The thermal or near-thermal electron attachment rate (k_f) for SF_6 has been measured in several different types of experiments including electron-swarm,[42,43] flowing afterglow,[44] and ion cyclotron resonance.[41] Some of these results have been summarized and, except for two particularly low values, yield an average rate of 8.8×10^9 $sec^{-1} \cdot torr^{-1}$.[43] In two experiments temperature variability was possible and measurements indicated that the electron capture rate of SF_6 is independent of temperature between 0 and 200°C.[42,44]

Table 2.

Isotope shifts for the ν_3 band of SF_6

Sulfur Isotope	Natural Abundance (%)	$\nu_3(cm^{-1})$ Brunet & Perez[37]	Klimov & Lobikov[38]
^{32}S	95.06	947.9	947
^{33}S	0.74		939
^{34}S	4.18	930.5	930
^{36}S	0.0136		914

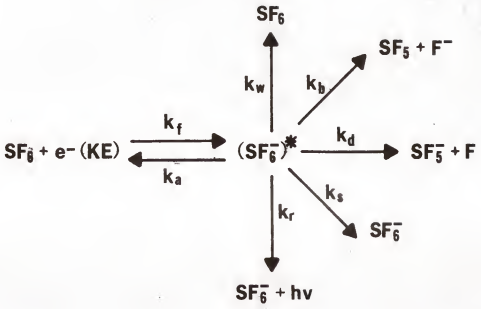

Figure 4. Kinetic diagram describing the reaction of SF_6 with electrons.

Assuming a v^{-1} dependence for the cross section, where v is the electron velocity, the measured attachment rates were used to calculate the capture cross section, yielding values between 10^{-15} and 10^{-14} cm^2.[42,44] Through a more comprehensive treatment of electron-swarm data, it was possible to determine both the magnitude and energy dependence of the subthermal electron attachment cross sections.[43] Results of these calculations indicated that the electron attachment cross section for SF_6 peaks for 0 eV electrons and rapidly decreases for increasing electron energy, in agreement with well-established experimental results.[45,46] Computed values varied from 5.4×10^{-15} cm^2 for an electron energy of 0.1 eV to 2.0×10^{-14} cm^2 for 0.03 eV electrons, implying that discrepancies in measured cross sections may reflect uncertainties in the electron energy. It has been pointed out that the experimentally determined cross sections for the attachment of low energy electrons to SF_6 approach the theoretical maximum of s-wave capture, which is 3.6×10^{-14} cm^2 at room temperature.[42,47]

After attaching an electron, the $(SF_6^-)^*$ complex may exist for considerable time before autoionizing, decomposing, or stabilizing. The value for the autoionization or autodetachment lifetime is still in question. Using a time-of-flight (TOF) mass spectrometer, it has been estimated to be $\sim$ 25 μsec in two experiments[42,46] and 68 μsec in another.[48] Analysis of ion cyclotron resonance (ICR) linewidths of SF_6^- and SF_5^- yielded a value $\geq$ 500 μsec.[49] This latter result prompted a re-examination of the autoionization process in an ICR experiment, establishing an upper limit of 0.3 to 2.0 msec for the lifetime.[50] It

has been suggested that discrepancies between different TOF measurements or between TOF and ICR measurements may be due to differences in the total energy of the $(SF_6^-)^*$ complex.[48,50] It has been pointed out that $(SF_6^-)^*$ ions, even when formed by monoenergetic electrons, will have a range of energies reflecting the thermal distribution of the original neutral molecules.[51] This makes it unlikely that a unique value for the lifetime can be determined. This argument is supported by Figure 5 which illustrates the internal energy distribution of neutral SF_6 at 300^oK.[52] It has been estimated that at this temperature about 30% of the molecules are in the first vibrational level.[41] Calculations indicate that changes in the total excess energy of the complex from 0.01 eV to 0.1 eV above threshold will cause the autodetachment lifetime to change by an order of magnitude.[51] Since the original thermal vibrational energy and the energy acquired on electron attachment are equivalent,[52] an additional source of error would be small changes in the average energy of the attaching electrons which could produce substantial changes in the total excess energy and appear as large changes in the ion lifetimes.

An interesting implication of the internal energy distribution argument given above pertains to electron capture characteristics of vibrationally excited SF_6. An experimental examination of electron attachment at low energy has indicated that for SF_6 the cross section for total ion production is temperature independent.[53] This leads to the conclusion that all initial vibrational states of SF_6 have the same cross section for electron capture near zero energy. However, two separate temperature controlled experiments have revealed that the

Figure 5. Internal energy distribution of neutral SF_6 at 300°K.

species of negative ions--SF_6^-, SF_5^-, or F^---formed by attachment of electrons of near zero energy depends strongly on temperature. This would indicate that the decay channels of the compound state; that is, branching ratios, are dependent on temperature.[44,54] An example of the temperature dependence for species formation is given in Figure 6[44] which shows the ratio of SF_5^- to SF_6^- as a function of temperature. An explanation of these results rests on the proposition that there is one common electronic complex $(SF_6^-)^*$ initially formed and that the branching ratios for dissociation of this complex depend on the initial internal energy of the SF_6 neutral. Additional insight into the nature of this complex was supplied by a theoretical investigation of the electronic properties of SF_6 which suggested that the production of SF_5^- results from the vibrationally excited ground electronic state $^2A_{1g}$ of SF_6^-.[55] Finally, the observed temperature dependence of the SF_5^- production and the assumption of temperature-dependent branching ratios were theoretically confirmed by rate constant calculations for autoionization and dissociation as a function of SF_6^- internal energy.[51,56] Results indicated that for internal energies greater than ~ 0.45 eV dissociation ($SF_5^- + F$) dominates autoionization.

An important gauge of the ability of an atom or molecule to capture and hold an electron is its electron affinity (E.A.) and significant effort has been made to determine the values for SF_6 and SF_5. Early measurements using the magnetron technique resulted in electron affinities of 1.4 and 3.6 eV for SF_6 and SF_5, respectively.[57] Monitoring reactions in a flowing afterglow, it was observed that SF_6^- charge transfers with atomic oxygen, whereas O_2^- charge transfers with

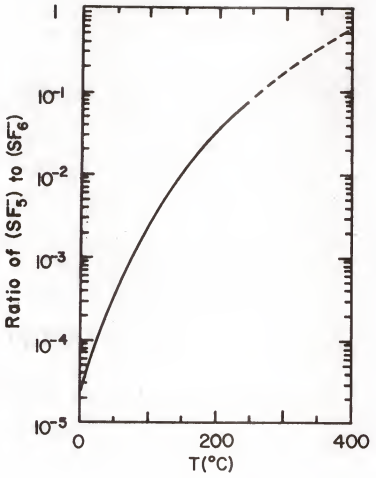

Figure 6. Temperature variation of the SF_5^- to SF_6^- ratio from 0 to 400°C. The solid line is taken from Reference 44 and the dotted line is an extrapolation of those data.

SF_6.[58] Since the electron affinities of O and O_2 have been established, it is possible to bracket the electron affinity of SF_6; that is, 0.43 eV < E.A. (SF_6) < 1.465 eV, which lends support to the above value of 1.4 eV for SF_6. A calculation of the electron affinity based on the experimentally determined SF_6 capture cross section and $(SF_6^-)^*$ lifetime yielded a value of 1.1 eV;[42] and in fact, it was noted that using a capture cross section as measured in another experiment the calculation gave 1.4 eV which is in close agreement with the measured value.

More recently, examination of charge transfer absorption spectra for SF_6 dissolved in tetrakis (dimethylamino) ethylene has resulted in an assignment of 0.6 eV for the SF_6 electron affinity.[59] However, it was pointed out that information on electron affinities obtained in this manner pertains to vertical transitions, which is a transition from the v = 0 level of SF_6 to the SF_6^- curve without a change in radial coordinate. A method has also been developed to determine electron affinities from the energy threshold behavior of cross sections for charge transfer reactions.[60] Applications of this technique to charge transfer from atomic negative ions to SF_6[61] and to collisional ionization of cesium by SF_6[62] have resulted in values of > 0.6 eV and > 2.8 eV for the electron affinities of SF_6 and SF_5, respectively. It has been acknowledged that electron affinities obtained in this manner are, strictly speaking, lower limits.[61] Based on the previous discussion and these observations, it seems reasonable to assume that the electron affinities of SF_6 and SF_5 are indeed $\sim$ 1.4 eV and $\sim$ 3.6 eV and that the values $\sim$ 0.6 eV (SF_6) and 2.8 eV (SF_5) represent vertical attachment

energies (V.A.E.).

Taking the SF_6 electron affinity as 1.4 eV, the bond dissociation energy, $D_o(SF_5 - F)$ has been calculated to be 3.7 eV.[57] A calculation based on the SF_5^+ appearance potential in a flowing afterglow has yielded a lower limit of 3.2 eV for this energy, which is close to the 3.3 eV value obtained from the heat of formation of SF_6.[63] All of these values are probably within the experimental error; however, the larger value is consistent with the assumed electron affinities and, as will be shown, conforms well to a proposed potential energy diagram. The electron affinities of SF_6 and SF_5 are taken to be 1.4 and 3.6 eV, respectively and the SF_6 bond dissociation energy to be 3.7 eV. The bond dissociation energy for SF_6^-, $D_o(SF_5^- - F)$, then becomes 1.5 eV.

In charge transfer experiments the difference in thresholds for the production of SF_6^- and SF_5^- have been determined with some accuracy; reported values for this difference are 1.05,[62] 1.1,[61] and 1.14 eV.[64] For convenience an average value of 1.10 eV will be taken for this quantity. This value has been interpreted to be the dissociation energy for SF_6^-;[64] however, as will be shown later, there may be an alternate explanation to the threshold difference (T.D.). The threshold difference for F^- production in collisional ionization of cesium by SF_6 has been shown to be ~ 1.75 eV.[62] Through the use of a potential energy diagram, this will be correlated with the observations that in temperature-controlled experiments F^- is not detected below $\sim 500^oK$.[44,54]

Another significant quantity which has been measured experimentally is the activation energy (A.E.). This is the energy required for a

system to pass from one state to another; in the present case it is the energy necessary to produce SF_5^- from SF_6^-. An Arrhenius plot of rate data from a flowing afterglow experiment indicated that the activation energy, A.E. (SF_5^- - F), is 0.43 eV.[44] This is in good agreement with values obtained in charge transfer experiments--0.51 eV,[62] 0.5 eV,[61] 0.39 eV[64] and the value measured in attachment of low energy electrons, 0.38 eV.[54] An average of these gives an activation energy of 0.45 eV.

Potential Energy Diagram

In an attempt to correlate the above results a potential energy diagram was constructed. In developing these potentials attention was focused on an S-F bond, which is equivalent to taking a cross section of the potential surface. It was assumed that the potential energy of this bond could be described by a Morse function[65] given by

$$U(r-r_e) = D_e \left\{1 - \exp\left[-\beta(r-r_e)\right]\right\}^2 , \qquad (1)$$

where r is the bond distance, r_e is the equilibrium bond distance, and D_e is the dissociation energy referred to the minimum. The quantity β is a constant whose value is

$$\beta = \sqrt{\frac{2\pi^2 c \mu}{D_e h}}\ \omega_e = 1.2177 \times 10^7\ \omega_e \sqrt{\frac{\mu_A}{D_e}} , \qquad (2)$$

where ω_e is the vibration frequency, μ_A is the reduced mass in atomic-weight units (Aston scale), and D_e is in cm^{-1}. The reduced mass was calculated by taking the fluorine atom as one mass and the sulfur atom plus the additional five fluorines as the other mass.

For SF_6 the equilibrium bond distance, r_e, was taken to be 1.56 Å.[66] A value of 3.7 eV[57] was assigned to D_e. It is recognized that the quantity measured in experiments is D_o, the dissociation energy referred to the zero vibrational level; however, the zero level is only ~0.05 eV above the minimum so that this assignment is well within experimental error. In this representation the S-F bond is an idealized bond. One approximation to this bond frequency, based on a group frequency argument,[34] is to assume that ω_e is a weighted average of the three fundamental frequencies in SF_6 which represent pure S-F stretching motion; that is,

$$\omega_e = \frac{1}{6} (\nu_1 + 2\nu_2 + 3\nu_3) , \qquad (3)$$

where ν_1, ν_2, and ν_3 are listed in Table 1. The weighting factors 1, 2, and 3 represent the degeneracy of each vibration mode. Using the frequencies in the first column of Table 1 yields a value of 811.17 cm^{-1} for ω_e.

Indications are that the orbital accepting the additional electron in SF_6^- is antibonding in character.[59] If this were concentrated in a single bond, it would produce a 50% reduction in the bond strength. However, it is assumed that the reduction is spread over six S-F bonds, resulting in a decrease of ~8% for any one bond. As a consequence of this, the bond length increases and the vibrational frequency correspondingly decreases. To ascertain appropriate r_e and ω_e values for SF_6^-, upper and lower limits--listed in Table 3 along with the SF_6 values--were taken for each. Assuming D_e to be 1.5 eV,[44] four potential

Table 3.

Parameters for the SF_6 and SF_6^- potential energy curves

	D_e(eV)	r_e(Å)	ω_e(cm^{-1})
SF_6	3.7	1.56	811.17
SF_6^-	1.5	1.66	573.58
	1.5	1.66	740.49
	1.5	1.86	573.58
	1.5	1.86	740.49

curves were generated for SF_6^- by taking all possible combinations of r_e and ω_e. These curves were overlayed on the SF_6 curve and adjusted until their asymptotes were separated by 3.6 eV,[57] the electron affinity of SF_5. Selection of the proper curve was based on the criterion that it cross the SF_6 curve at about the SF_5^- activation energy~0.45 eV. This resulted in values for r_e and ω_e of 1.66 Å and 740.49 cm^{-1}, respectively. The curves generated in this manner are illustrated in Figure 7.

The ground state electronic configuration for SF_6 is $^1A_{1g}$ and for SF_6^- is expected to be $^2A_{1g}$.[62] A repulsive SF_6^- state leading to SF_5 and F^- dissociation products is also indicated in Figure 7; it is assumed to be a $^2A_{1g}$ state. Ordinarily this state, which corresponds to a small negative F ion being brought into a polarizable SF_5 group, would form a stable bond, resulting in a curve with a deep minimum. Likewise, the SF_6^- ground state, which is derived from a small neutral atom--F--being brought into a large ionic group--SF_5^-, would form a less stable bond, resulting in a flatter curve. However, because these two curves have the same symmetry, there is an avoided crossing producing a repulsive curve with a shallow minimum. The point of the avoided crossing is indicated by dotted lines in the diagram. The asymptote for the repulsive curve, which leads to SF_5 and F^- dissociation products, is taken to be 3.45 eV below the (SF_5 - F) dissociation limit. This energy--3.45 eV--equals the electron affinity of fluorine.[67] This would seem to lend support to the values chosen for the dissociation energies and electron affinities. Smaller values for these quantities

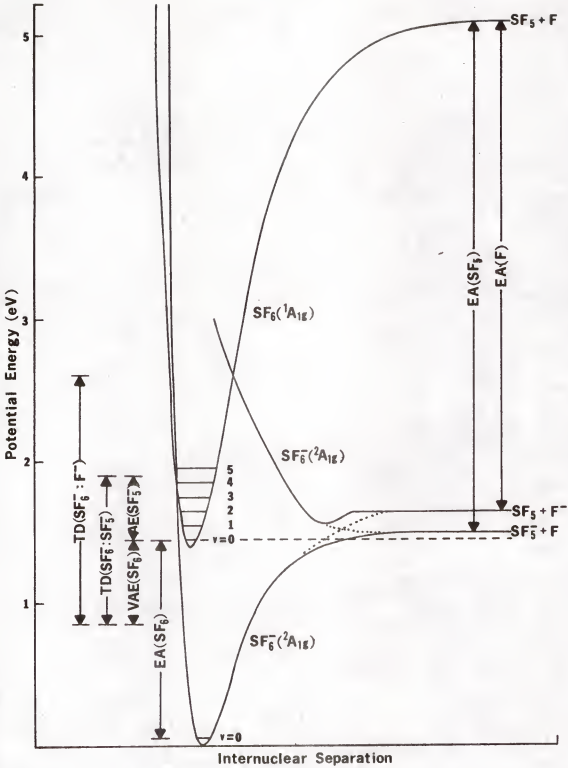

Figure 7. Potential energy curves for SF_6 and SF_6^-.

would put the ($SF_5 - F^-$) dissociation limit below the ($SF_5^- - F$) limit, creating an unacceptable configuration. It should be pointed out that there may be other excited states (^2E) which parallel the $^2A_{1g}$ states and converge to the same dissociation limits.

Ignoring anharmonic effects, the first five vibrational levels of the SF_6 ground state and the zero vibrational level of the SF_6^- ground state were calculated by

$$G(v) = \omega_e(v + \tfrac{1}{2}) \ , \qquad (4)$$

where G is the term value, ω_e the vibration frequency, and v is the vibration quantum number. This places the zero level of SF_6 at 0.05 eV from the minimum with the succeeding levels equally spaced 0.1 eV apart. The zero level of SF_6^- occurs at 0.046 eV. The approximate positions of these levels are indicated in Figure 7.

Careful examination of the potential energy diagram lends support to some previous assumptions about and provides explanations for the experimentally measured quantities. As was pointed out earlier, the well-established electron affinity of fluorine at 3.45 eV justifies choosing 1.4 eV and 3.6 eV as the electron affinities of SF_6 and SF_5. This in turn supports the values 3.7 eV and 1.5 eV for $D_o(SF_5 - F)$ and $D_o(SF_5^- - F)$, respectively. With the SF_6 and SF_6^- ground states constructed in this fashion, the energy for a vertical transition is 0.6 eV. This is identified as the SF_6 vertical attachment energy, V.A.E.(SF_6), and corresponds exactly to the value measured in charge transfer experiments. The SF_5^- activation energy, A.E. (SF_5^-), was

chosen such that the attractive potentials crossed at a point ~ 0.45 eV above the $v = 0$ level of SF_6. This places the curve crossing at about the fourth or fifth vibrational level in agreement with earlier work.[44] The threshold difference for SF_6^- and SF_5^-, T.D. (SF_6^- & SF_5^-), is measured from the point at which the vertical crosses the SF_6^- curve to the point at which the SF_6 and SF_6^- ground states cross. This yields an onset difference of 1.1 eV in accord with experimentally measured values. It is interesting to note that the SF_6^-, SF_5^- onset difference is approximately equal to the sum of the vertical electron affinity and the activation energy. This is reasonable since the fourth or fifth level can be populated either thermally or collisionally; attachment of an electron would then result in an energy greater than the dissociation causing a dissociation into SF_5^- and F. Finally, the threshold difference for SF_6^- and F^-, T.D. (SF_6^- & F^-), is measured from the point at which the vertical crosses the SF_6^- attractive curve to the point at which the SF_6^- repulsive curve crosses the SF_6 curve. This value is reported to be 1.75 eV.[62] If the SF_6 molecule is raised to a high vibration level ($v \sim 12$) either thermally or collisionally, the attachment of an electron will result in dissociation to SF_5 and F^- via the repulsive curve.

Two other potential energy diagrams have been suggested to explain the experimental results.[44,61] However, in neither case was the $SF_5 - F^-$ dissociation limit taken into account; that is, no allowance was made for the electron affinity of the fluorine atom. In addition only part of the experimental observations could be accounted for. It is felt

that the present potential energy curves represent an improvement, since care was taken in adjusting them. Their justification rests on the fact that they incorporate more experimental information. It should be pointed out that these curves could have been generated using other values for the vibration frequency. For example, ν_3 could have been used instead of the weighted average. When this was done, it was found that to obtain a proper crossing at $\sim v = 4$ required shifting r_e for SF_6^- to values approaching r_e for SF_6. It is understood that the percentage reduction in the bond due to the antibonding character of the added electron is only approximate. Nevertheless, the shifting of r_e for SF_6^- to lower values seemed to negate the antibonding argument and lend support to the assumption of frequency averaging.

CHAPTER III

ELECTRON ATTACHMENT MECHANISM

A mechanism for isotope separation which incorporates the electron attachment properties of the molecule and selective excitation by the laser can be visualized using the potential energy diagram developed in the last chapter. Recall that the original internal energy of a neutral molecule is carried over to the parent ion. Suppose a sample of gas having its natural isotopic abundance is irradiated by a laser tuned to an absorption line of only one isotope. This isotope will be vibrationally excited and attachment of an electron at this instant will produce a vibrationally excited ion. If the internal energy of the ion exceeds the dissociation energy, then it is possible for this ion to dissociate into products which may react chemically to form new species. The net result is a removal of one isotope and a corresponding enrichment of the other isotopes in the sample.

Application of this process requires that the molecule have certain properties. First, it must readily absorb the laser radiation and the spectral isotope shifts must be large enough that there is no overlap in the absorption lines of different isotopes. It is equally important that the electron affinity be less than the negative ion dissociation energy. Since electron attachment is not selective, electrons will

attach to both the laser designated isotope and the other isotopes. If the electron affinity were greater than the dissociation energy, then all the molecules would dissociate,not just the laser excited ones. Finally, it is beneficial if there is no charge exchange between the negative parent ion of one isotope and the neutral molecule of another isotope. Any charge exchange before dissociation would reduce the overall efficiency of the process.

A molecule particularly suited to this separation mechanism is sulfur hexafluoride. The ν_3 band of this molecule strongly absorbs various lines of the CO_2 laser as has been verified by a study of the ν_3 temperature-dependent absorption spectrum.[68] As was indicated in Table 2, isotope shifts for SF_6 are sufficiently large that only the desired isotope will be excited. From Figure 7 it can be seen that the electron affinity is slightly less than the SF_6^- dissociation energy. Finally, it has been shown that there is no charge exchange between $^{32}SF_6^-$ and $^{34}SF_6^-$.[61]

To illustrate the use of this technique for separating sulfur isotopes, consider a sample of SF_6 having the natural isotopic abundance of sulfur--95% ^{32}S and 4% ^{34}S. Suppose a CO_2 laser is tuned to an absorption line in the ν_3 band of $^{32}SF_6$ and that this constituent is saturated by the pulse. Absorption of this radiation will increase the vibrational energy of $^{32}SF_6$ above that of $^{34}SF_6$. The frequency of collisions between $^{32}SF_6$ and $^{34}SF_6$ will be low, since $^{34}SF_6$ is only 4% of the initial sample. The absorbed energy may be equilibrated among the $^{32}SF_6$ molecules via V-V collisions, but transfer to $^{34}SF_6$ should be

negligible. Note, however, that as the sample is enriched by the removal of $^{32}SF_6$ this collision frequency will increase and V-V exchange between the two isotopic species may become important. It is assumed that all the molecules in the sample have the same initial vibrational distribution so that absorption of the laser radiation will strongly enhance the population of the lower vibrational levels. Due to the curve crossing at the fourth vibrational level indicated in Figure 7, electron attachment will result in a complex, $(^{32}SF_6^-)^*$, whose internal energy is much greater than the SF_5^- + F dissociation energy. The net effect will be a greater production of $^{32}SF_5^-$ than $^{34}SF_5^-$. If the SF_5^- ions react chemically to form a stable compound, this compound will have a greater than natural abundance of ^{32}S, leaving the gaseous SF_6 enriched in ^{34}S.

The efficiency of this process could be calculated if detailed information were available for both the collisional V-V rates for population of vibrational levels and the SF_5^-/SF_6^- branching ratio as a function of the initial vibrational level. Lacking this information, a rough estimate of the efficiency can be made, based on the temperature dependence of the SF_5^-/SF_6^- branching ratio previously presented in Figure 6. Use of this branching ratio depends strongly on the equivalence of thermal energy and energy acquired through collision or photon absorption. The vibrational energy gained through absorption is equated with a temperature and the branching ratios for the original temperature and the new temperature taken from the diagram. For example, assume that as a result of laser action on $^{32}SF_6$ the difference in internal

energy between it and $^{34}SF_6$ is equivalent to 330°C. If the sample was at 20°C originally, then the $^{34}SF_6$ will remain at 20°C and the $^{32}SF_6$ will be raised to 350°C, corresponding to branching ratios of 7.0×10^{-5} and 0.35, respectively. Employing the natural abundance of the two isotopes and recalling that no scrambling occurs, these ratios yield relative fractions of 2.8×10^{-6} for $^{34}SF_5^-$ and 0.316 for $^{32}SF_5^-$. Any compound formed from SF_5^- will then have a ^{32}S to ^{34}S ratio of 1.13×10^5 which represents an increase of 4760 over the natural ratio of 23.75. The remaining gas is correspondingly reduced in ^{32}S content.

If the laser is focused and operated just below breakdown threshold, the electrons necessary for dissociation can be produced by ionization of SF_6 yielding SF_6^+. However, SF_6^+ is unstable and decomposes to SF_5^+ and F,[58] which in combination with SF_5^- could yield S_2F_{10} as one of the products. Since the $^{32}SF_5^-$ ions are free to combine with either $^{32}SF_5^+$ or $^{34}SF_5^+$, the enrichment factor of ^{32}S in disulfur decafluoride would be reduced.

The dissociative electron attachment method is appealing since it requires absorption of only a few photons by and an electron attachment to the reacting molecule. By using an external electron source the required laser power may be reduced compared to that necessary for separation with the focused beam method. In fact, this technique may permit isotope separation with an unfocused or even expanded beam which would facilitate processing of larger quantities of material. For this scheme to be successful, it is necessary that electron attachment and dissociation occur before the excited molecule has been deactivated by

molecular and wall collisions or autodetaches its electron. Compensation for these loss mechanisms requires a high attachment rate and that the dissociation rate be greater than the autodetachment rate. Calculations of rate constants for unimolecular decomposition at threshold indicate that the latter condition will be met if the operating pressure is low.[56] Taking this into consideration, satisfaction of the former requirement of a high attachment rate requires a substantial electron density. For example, successful application of the technique to SF_6 would necessitate an operating pressure of approximately one torr. At this pressure nearly 10^{12} cm^{-3} zero-energy electrons would be required.

CHAPTER IV

EXPERIMENTAL EFFORTS

Duplication of Reported Experiments

Upon learning about the success of separating isotopes using only the focused radiation of a CO_2 TEA laser,[22,23] it was decided to attempt duplication of those experiments. A Lumonics CO_2 TEA laser (Model TEA-101-1) similar to the one used at Los Alamos[23] was available in the laboratory. When operated on a mixture of He, CO_2, and N_2 in the ratio 8:2:1, this laser emits a 5 joule pulse in 250 nsec yielding a peak power of 20 MW. Since the cavity is not tuned, lasing occurs on the P(20) line of the $00^01 - 10^00$ transition in CO_2. As was pointed out in Chapter II, this radiation, having a wavelength of 10.59 μm, is readily absorbed by the ν_3 band of $^{32}SF_6$. In fact, an investigation of the temperature-dependent absorption spectrum of this band indicated that at 300^oK the P(20) line has one of the highest absorption coefficients, 9.75×10^6 $(mol/cm^3)^{-1}$ cm^{-1}.[68]

A Pyrex cell with an approximate volume of 150 cc was equipped with salt flats to pass the laser radiation. The beam was focused in the cell with an f/5 germanium lens which had a one-inch free aperture. The laser operates multimode producing a pillow-shaped pattern which overfills the focusing lens. To prevent damage to the lens holder the beam was apertured to one inch before being focused. This results in some energy loss from the beam. Since only a fraction of the beam

energy is absorbed by the gas, a block was placed behind the cell to act as a beam dump. The experimental set up is indicated in Figure 8.

The gas cell was initially evacuated to a pressure of approximately one micron and then filled to one torr with SF_6 in its natural isotopic composition. Before irradiation samples were taken for mass and infrared analysis. The cell was again evacuated and refilled to a pressure of one torr. This gas was then irradiated by 3300 pulses from the laser and samples taken for analysis.

The natural sample and the pulsed sample were analyzed with a Perkin-Elmer El infrared spectrometer. The results of scans around the 10.6 μm region are shown in Figure 9. The sloping line indicates the baseline of the instrument. Initially, the $^{34}SF_6$ peak is dwarfed by the $^{32}SF_6$ peak; however, after irradiation with the laser, the two features are near the same height. This indicates that $^{32}SF_6$ has been removed during irradiation, the net result being an enrichment in $^{34}SF_6$. Note that the $^{34}SF_6$ peak remains constant, implying that this constituent is unaffected by the process. These conclusions were confirmed by mass analysis.

Electron Gun Experiment

To experimentally verify the dissociative electron attachment mechanism, an electron gun was constructed to serve as a source of thermal electrons. Essentially a triode in design, the gun consisted of a rhenium ribbon filament heated by a six ampere dc current, a tungsten wire mesh grid, and a collector plate. Several guard plates were also included in the assembly. Two dc power supplies were used to

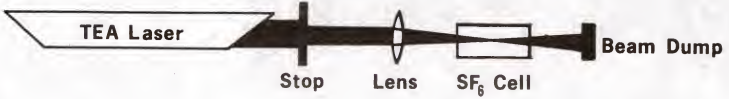

Figure 8. Experimental set up for separation of isotopes using the focused beam method .

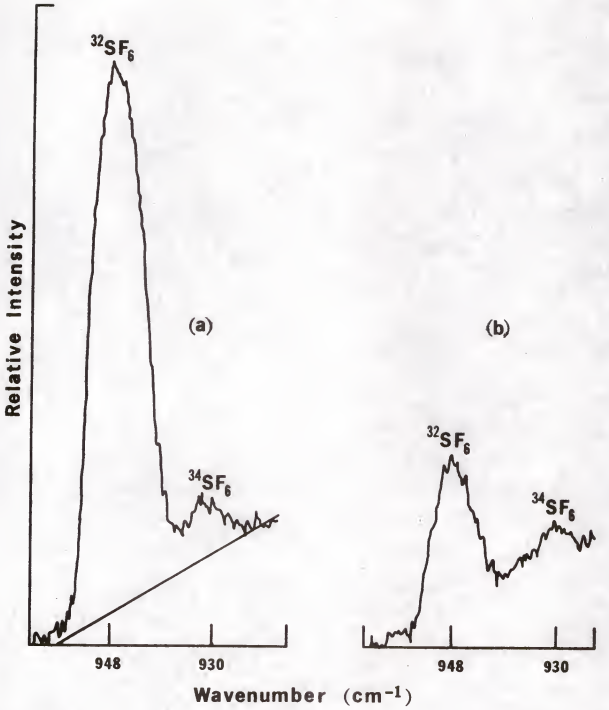

Figure 9. Infrared spectra of SF_6. (a) Natural sample (b) Laser pulsed sample.

regulate the grid and collector plates. The grid voltage, plate voltage, and plate current were monitored with digital voltmeters. The spacing between the grid and the plate was chosen to accommodate the laser beam either focused or unfocused. The whole assembly was fitted into a tee-shaped Pyrex cell with ample ports for pumping and filling. The cell was equipped with salt flats to permit entry of the laser beam. The experimental set up is identical to that in Figure 8 with the electron gun cell substituted for the gas cell.

A natural sample of SF_6 was drawn through the cell to serve as a reference. The cell was then filled with one torr of SF_6, the filament turned on, and the laser switched on. However, before a run could be completed the rhenium filament broke. The filament was replaced and the experiment repeated, but each time the result was the same. It was noticed that the filament increased the temperature of the cell considerably. It is presumed that destruction of the filament was caused by a reaction of the hot SF_6 with the hot rhenium similar to the one reported for tungsten;[69] that is,

$$3SF_6 + Re \rightarrow ReF_6 + 3SF_4 \ . \qquad (5)$$

Experiments using this technique were discontinued.

Pulsed Hollow Cathode Experiments

A second attempt was made to obtain experimental evidence of the dissociative electron attachment mechanism. It was decided to use a pulsed hollow cathode as the electron source. This was desirable because the hollow cathode discharge is a cold one eliminating the

unwanted heating effect of the filament which altered the vibrational distribution of the SF_6 molecules. A second advantage of the hollow cathode was pulsing, since the laser and the discharge could now be coordinated. By using time delays it was possible to produce the electrons before, during, or after the laser pulse.

To construct the hollow cathode, the end flanges of a 50 cm^3 tee-shaped cell were machined with a hollow cylinder one-half inch in length. These cylinders just fit inside the cell. Centered in the middle of the cell three quarters of an inch equidistant from either end was another hollow cylinder. The two end flanges, which also accommodated the salt flats, were electrically grounded. An 0.02 mfd capacitor was charged to 10 kV and then discharged through a gas switch, placing the center cylinder at -10 kV. This produced a glow between the cylinder and the end flanges. Connection of the gas switch through a spark coil to a pulse unit permitted repetitive firing of the hollow cathode.

First, a sample of natural SF_6 was drawn through the cell to serve as a reference. Then the cell was filled to 1.50 torr with SF_6 and this sample was subjected to 900 laser pulses producing a known enrichment in the gas. With the same sample still in the cell, the hollow cathode was pulsed 900 times and a portion drawn off for infrared analysis. The cell was evacuated and refilled to 1.50 torr. This time the order was reversed--first the hollow cathode was pulsed 900 times and then the laser for 900 times. Again a sample was drawn for infrared analysis. The gas samples were analyzed with a Beckman IR10

infrared spectrometer. These scans appear in Figure 10 as (a) the natural sample, (b) the hollow cathode-laser sample, and (c) the laser-hollow cathode sample. From Figure 10(c) it appears that the hollow cathode destroys any enrichment that was achieved with the laser; that is, the hollow cathode scrambles the separated isotopes. An interesting aspect of the hollow cathode-laser sequence as illustrated in Figure 10(b) is that it gave a high enrichment value. This implies that the hollow cathode must prepare the gas in some way favorable to the laser enrichment process.

It was apparent from these tests that the hollow cathode could not be used as the electron source, since each pulse with the hollow cathode would destroy any separation which might have been produced by dissociative electron attachment. As a result it was decided to seek experimental verification using an ion cyclotron resonance apparatus. This aspect of the research will be discussed in the next chapter.

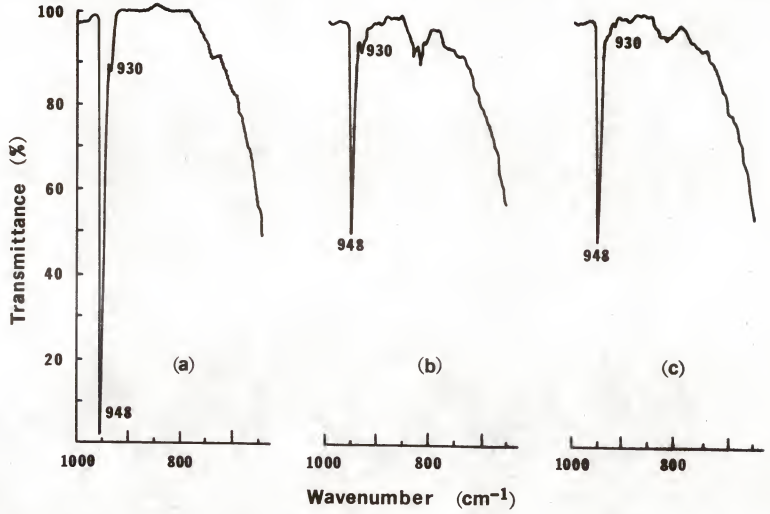

Figure 10. Infrared scans of SF_6. (a) Natural sample (b) Sample processed by the hollow cathode, then the laser (c) Sample processed by the laser, then the hollow cathode.

CHAPTER V

ION CYCLOTRON RESONANCE PROGRAM

An ion cyclotron resonance (ICR) apparatus has the capacity to trap ions for long periods of time. Such a piece of equipment was available for use and though its resolution was not sufficient to distinguish between $^{32}SF_6^-$ and $^{34}SF_6^-$, it could differentiate between SF_6^- and SF_5^-. An experiment was designed using the ICR machine in conjunction with the CO_2 TEA laser in an attempt to provide indirect proof of the dissociative electron attachment process. The ICR cell was fitted with a window so that the laser radiation could be introduced. The laser pulse, which would excite the SF_6, was to be followed by a burst from the electron gun. Dissociative electron attachment should then be observed as an increase of SF_5^- production over that detected during normal operation; that is, with no laser excitation. To guide the experiments, a kinetics model was developed and the appropriate set of reaction rate equations solved numerically on the I.B.M. 360-75 computer at the University of Florida. The reaction scheme was depicted earlier in Figure 4. Results from another ICR experiment[41] supported assumptions concerning reaction rates and duplication of these experimental results by the kinetics program suggested that the model was a reasonable one.

Kinetics Model

Description of the kinetics scheme was accomplished using thirteen

reactions--six reactions for unexcited SF_6, six similar reactions for laser-excited SF_6, and a wall deactivation reaction for the laser-excited molecules. These reactions and their corresponding rate symbols are listed in Table 4. Reference can be made to Figure 4 for assistance in visualizing the various channels. Reactions 1, 2, and 11-13 are bimolecular reactions whose rates are dependent on number density; the remaining reactions are unimolecular.

These thirteen reactions were characterized by eight rate equations which described the time development of the number density for eight different constituents. When non-dimensionalized with respect to the initial SF_6 number density, these equations take the form

$$\frac{dn_1}{dt} = - k_w' n_1 + k_a' n_3 - k_f' n_1 n_8 \tag{6}$$

$$\frac{dn_2}{dt} = - k_a n_2 - k_b n_2 - k_d n_2 - k_r n_2 + k_f n_7 n_8 - k_s n_2 n_7 \tag{7}$$

$$\frac{dn_3}{dt} = - k_a' n_3 - k_b' n_3 - k_d' n_3 - k_r' n_3 + k_f' n_1 n_8 - k_s' n_3 n_7 \tag{8}$$

$$\frac{dn_4}{dt} = k_d n_2 + k_d' n_3 \tag{9}$$

$$\frac{dn_5}{dt} = k_r n_2 + k_r' n_3 + k_s n_2 n_7 + k_s' n_3 n_7 \tag{10}$$

$$\frac{dn_6}{dt} = k_b n_2 + k_b' n_3 \tag{11}$$

$$\frac{dn_7}{dt} = - \sum_{i=1}^{6} \frac{dn_i}{dt} \tag{12}$$

$$\frac{dn_8}{dt} = k_a n_2 + k_a' n_3 - k_f' n_1 n_8 - k_f n_7 n_8 \tag{13}$$

where the quantities n_i refer to the following constituents

Table 4.

Reactions and rate symbols for the kinetics model

Reaction	Rate symbol
1. $SF_6 + e \rightarrow (SF_6^-)^*$	k_f
2. $SF_6^+ + e \rightarrow (SF_6^-)^{**}$	k_f'
3. $(SF_6^-)^* \rightarrow SF_6 + e$	k_a
4. $(SF_6^-)^{**} \rightarrow SF_6^+ + e$	k_a'
5. $(SF_6^-)^* \rightarrow SF_5 + F^-$	k_b
6. $(SF_6^-)^{**} \rightarrow SF_5 + F^-$	k_b'
7. $(SF_6^-)^* \rightarrow SF_5^- + F$	k_d
8. $(SF_6^-)^{**} \rightarrow SF_5^- + F$	k_d'
9. $(SF_6^-)^* \rightarrow SF_6^- + h\nu$	k_r
10. $(SF_6^-)^{**} \rightarrow SF_6^- + h\nu$	k_r'
11. $(SF_6^-)^* + SF_6 \rightarrow SF_6^- + SF_6$	k_s
12. $(SF_6^-)^{**} + SF_6 \rightarrow SF_6^- + SF_6$	k_s'
13. $SF_6^+ + M \rightarrow SF_6 + M$	k_w'

Note: + denotes a laser-excited molecule, * denotes a complex formed from an unexcited molecule, ** denotes a complex formed from a laser-excited molecule. k' refers to rates involving laser-excited molecules.

$n_1 : SF_6^+$

$n_2 : (SF_6^-)^*$

$n_3 : (SF_6^-)^{**}$

$n_4 : SF_5^-$

$n_5 : SF_6^-$

$n_6 : F^-$

$n_7 : SF_6$

$n_8 : e$

Note that Equation (12) is essentially a conservation equation for SF_6.

Numerical solutions to these rate equations were obtained using Hamming's modification of the Milne predictor-corrector method. It is not self-starting; that is, the values at a single previous point are not enough to get the values ahead. Therefore, a special Runge-Kutta procedure is used to generate the starting values. The Hamming routine is a stable fourth-order integration procedure which requires fewer evaluations per step than other methods of comparable accuracy. This reduces computing time without affecting the accuracy. An additional advantage is that the procedure is able to choose and change step size. In applying this routine to these equations the accuracy was specified to one part in 10^4 and the time step was 0.5 units, one unit being one millisecond. To obtain the specified accuracy the time step could be bisected up to ten times.

The apparent bimolecular rate constant for electron attachment was determined in another ICR experiment to be 1.6×10^{-8} cm^3 molecule^{-1}

sec^{-1}.[41] This value is an order of magnitude smaller than those measured in other types of experiments.[44] Therefore, in the program the attachment rates k_f and k'_f were set equal to 10 k_{app}. Use of the same rate for electron attachment to excited and unexcited SF_6 is supported by experimental observation.[53] Rates k_s and k'_s, which represent collisions of excited negative ions with their parent neutrals, were estimated from the ion-induced collision rate given by[70]

$$k_s = 2\pi e(\alpha/\mu)^{\frac{1}{2}} = 7.00\text{x}10^{-10}\ cm^3\ molecule^{-1}sec^{-1} \qquad (14)$$

where e is the electronic charge, α the polarizability of SF_6, and μ the reduced mass of the collision pair. It was assumed that this rate was independent of the vibrational level of the ion so that the same value could be taken for both k_s and k'_s. The wall collision rate was evaluated on the basis of the mean molecular speed at 300°K and the cell width. This resulted in a collision frequency of $10^4\ sec^{-1}$.

Relationships between some unimolecular rates were attained from the data reported in Reference 41. The negative-ion mass spectrum of SF_6 showed SF_6^- and SF_5^- in a ratio of approximately 20:1. This suggested that the ratio of the radiative rate to the SF_5^- - F dissociative rate was also approximately 20:1; that is, $k_r/k_d = k'_r/k'_d \sim 20$. The ratio of the autodetachment rate to the radiative rate was determined to be 10:1 by comparing the attachment rates for CCl_4 and SF_6 in low and high pressure experiments. In brief this means that $k_a/k_r = k'_a/k'_r \sim 10$. Results from the temperature-controlled experiments[44,54] indicated that the F^- production was 10% of the SF_5^- - F^- dissociation rate; that is, $k_d/k_b = k'_d/k'_b \sim 10$. From a theoretical treatment of electron swarm data[51]

it has been inferred that an excited SF_6 complex is ten times more likely to dissociate into SF_5^- and F than to autodetach an electron; that is, $k_d'/k_a' \sim 10$. Finally, it was assumed that the radiative rate was the same for the two complexes $(SF_6^-)^*$ and $(SF_6^-)^{**}$; the autodetachment rate was also assumed to be the same for both cases. It is necessary to have a value for one of the rates in order for these ratios to be useful. The production of stable SF_6^- in the low pressure trapped-ion experiment suggested a radiative process with a lifetime of several milliseconds.[41] In the present case this lifetime was assumed to be 5 msec, so that k_r takes a value of 200 sec^{-1}. The values for the other unimolecular rates resulting from this assumption are listed in Table 5.

Proper use of the bimolecular rates requires specification of the number density or equivalently the operating pressure. To duplicate the experimental results of Reference 41, the pressure was taken to be 1.5×10^{-7} torr. In addition, it was assumed that the electron number density just equaled the initial SF_6 number density. The bimolecular rates which were used in the program are also listed in Table 5.

Simulation of the ICR experiment with no laser excitation required setting the SF_6^+ number density, which is read in as an initial condition, equal to zero. The results for SF_6^- and SF_5^- production appear in Figure 11. For comparison the trapped-ion spectrum from an ICR experiment is reproduced in Figure 12.[41] The model predicted the ratio of SF_6^- to SF_5^- to be 20.2, as compared to the measured ratio of 20. Therefore, the program seems quite adequate and may be used with some degree of confidence.

Table 5.

Reaction rates for the kinetics program

Symbol	Rate (sec^{-1})
k_f	8.5×10^2
k'_f	8.5×10^2
k_a	2.0×10^3
k'_a	2.0×10^3
k_b	1
k'_b	2.0×10^3
k_d	10
k'_d	2.0×10^4
k_r	2.0×10^2
k'_r	2.0×10^2
k_s	3.7
k'_s	3.7
k_w	10^4

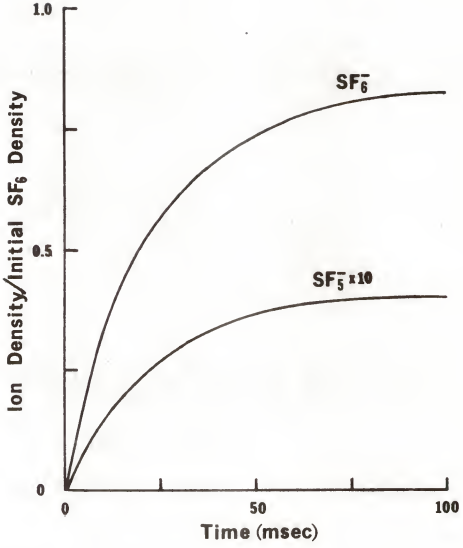

Figure 11. Production of SF_6^- and SF_5^- as determined by the kinetics program.

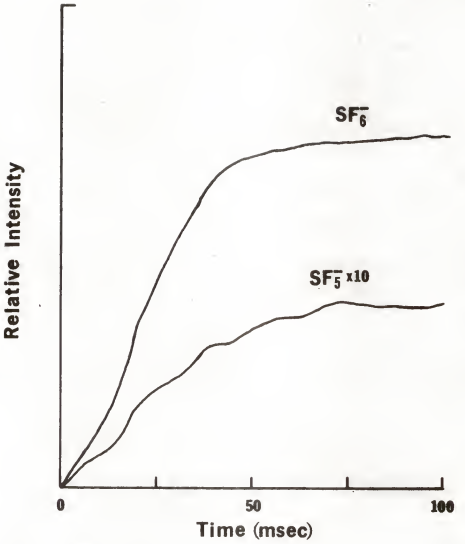

Figure 12. ICR trapped-ion spectrum for SF_6^- and SF_5^-.

Kinetics Model Predictions and Experimental Results

For the first case the cell pressure was again taken to be 1.5×10^{7} torr, so that the rates remained unchanged from the case for no laser excitation. It was assumed each laser pulse excited 1% of the molecules. The program predicted an SF_6^- to SF_5^- ratio of 20.4. This is essentially the same as the predicted and measured ratios for no laser excitation. It was concluded that due to the low pressure the laser-excited molecules quenched on the walls before an electron could be attached.

It was decided to try the experiment in spite of the fact that there was essentially no change predicted in the ratio. The SF_6 pressure in the ICR cell was held at 1.5×10^{-7} torr and the electron beam energy was nominally 70 volts. Each laser pulse made two passes through the cell, since a dielectric coated mirror was mounted at the rear of the cell. The laser, electron beam, and quench pulses were triggered from an oscilloscope and could be delayed with respect to one another. The experiment also gave a null result, as no change in the ratio was observed when the laser was on.

To increase the attachment rate and decrease the wall deactivation rate, the cell pressure was increased to 5×10^{-6} torr. This resulted in a value of 2.83×10^{4} sec^{-1} for the attachment rates and 124 sec^{-1} for the $SF_6 - SF_6^-$ collision rate. The wall collision rate was assumed to decrease an order of magnitude for this increase in pressure. The unimolecular rates remained unchanged. The program was first run with no laser excitation and yielded an SF_6^-/SF_5^- ratio of 21.8. When laser

excitation was introduced, it was assumed that 3% of the SF_6 molecules would be excited. Again the electron number density was set equal to the initial SF_6 number density. Based on these suppositions, the program predicted a value of 13.7 for the SF_6^-/SF_5^- ratio.

The predicted difference in SF_5^- production for this case was well within the detection capabilities of the ICR system. Therefore, the experiment was rerun at a pressure of 5×10^{-6} torr; the electron beam energy remained at 70 volts. The measured SF_6^-/SF_5^- ratio for no laser excitation was in good agreement with the predicted ratio. However, the laser did not have the desired effect as no change was detected when the gas was irradiated. This failure to achieve experimental verification in view of the model prediction may be attributed to several things. First, it is not clear that 3% of the SF_6 will be excited by each laser pulse. Likewise, the assumed value for the wall collision rate may be in error.

The use of a continuous wave laser would eliminate the wall deactivation problem, since molecules would continually be excited. Though such a laser was not available, it was decided to modify the program so that continuous excitation was incorporated. The modification was achieved by the addition of one reaction to the scheme;

$$SF_6 + h\nu \rightarrow SF_6^* \quad . \tag{15}$$

This was represented by the addition of the term $k_e(f\, n_7 - n_1)$ to the first rate equation, where k_e is the absorption rate and f is the fraction of SF_6 which is excited. A value of 2.0×10^6 sec^{-1} was taken

for k_e and again it was assumed that only 1% of the molecules would be excited. Likewise, the pressure was fixed at 1.5×10^{-7} torr and the wall collision rate at 10^4 sec^{-1}. On the basis of this information the modified model predicted an SF_6^-/SF_5^- ratio of 7.3. This represents a considerable change in SF_5^- production from the case of no laser excitation for which the ratio is $\sim$20.

Since a tunable cw CO_2 laser was not available, experimental verification was not possible. The ICR experiments were discontinued until the proper laser could be built. In the meantime attention was turned to measuring the intensity threshold for laser isotope separation which is treated in the Appendix.

CHAPTER VI

SUMMARY AND CONCLUSIONS

A mechanism for separation of sulfur isotopes has been proposed. It is dependent on the infrared absorption characteristics and electron attachment properties of sulfur hexafluoride. In this scheme the molecule containing the isotope to be removed is selectively excited by a CO_2 laser. If an electron attaches before collisional deactivation occurs, then a negative ion complex whose energy is greater than the dissociation energy may be formed. Fragments of the dissociation process can be removed chemically, leaving the gas phase isotopically enriched.

Potential energy curves for sulfur hexafluoride were generated to aid in explaining the mechanism. These curves represent an improvement over those previously reported.[44,61] Though based on a simple approach, they succeeded in explaining and reconciling many experimental observations of the electron attachment process for sulfur hexafluoride.

Several unsuccessful attempts were made to obtain experimental verification of the process. However, results from a computer model of the ion cyclotron resonance experiment indicated that using a continuous wave CO_2 laser the SF_6^-/SF_5^- ratio would be lowered to approximately 7. This would offer indirect proof of the mechanism, since the ratio for the case of no laser excitation is ~ 20.[41]

A continuous wave CO_2 laser was not available for the ion cyclotron

experiments, so an investigation of the threshold intensity dependence for isotope separation by the focused beam method was begun. A detailed discussion is presented in the Appendix. The theoretical analysis surprisingly indicated that the threshold intensity is dependent on the f/number of the focusing lens, a purely geometric quantity. In addition, the threshold intensity was found to vary linearly with the laser power. Experimental measurements of this intensity yielded an average value of 6.04 MW/cm^2. This effectively eliminates the dynamic Stark broadening[27] and dissociative electron attachment[26] mechanisms as explanations of isotope separation using only the laser.

Although the measured value for the threshold intensity excludes dissociative electron attachment as an explanation of the laser separation process, it does not eliminate it as a viable mechanism for isotope separation. The advantage of this process is the reduction in the laser power necessary for separation. However, it requires a high electron density and a low pressure environment. The cw CO_2 laser - ICR experiment should be pursued and extension of the mechanism to other polyatomic molecules, including uranium hexafluoride, should be investigated.

APPENDIX

THRESHOLD INTENSITY FOR LASER INDUCED ISOTOPE SEPARATION IN SULFUR HEXAFLUORIDE

As was pointed out in Chapter I, considerable attention has recently been devoted to the separation of isotopes in polyatomic molecules using the focused output of a high power CO_2 TEA laser.[18,22-24] For most experimental conditions laser peak power has been estimated[18,22-24] to be $\sim 10^9$ watts/cm^2 at the focus. Apparently, this number has been evaluated on the basis of the nominal laser pulse energy, the pulse width, and the geometric focal volume. Several mechanisms have been proposed to explain the isotope separation process. For example, one explanation is based on dynamic Stark broadening of absorption lines in the high field,[27] while another depends upon the production of free electrons in the vicinity of the focal spot.[26] Both of these suggestions are dependent on a high threshold intensity value ($\sim 10^8 - 10^9$ watts/cm^2).

In the next section a method is developed to measure the threshold intensity dependence in the isotope separation process. A UV preionized CO_2 TEA laser was used to separate isotopes in pure sulfur hexafluoride; that is, no scavenger was used. Infrared absorption measurements of the processed sample were made to determine reaction rates. The threshold intensity was then determined from the measured reaction rates.

Theoretical Considerations

Laser radiation is focused into a cell which contains SF_6 and whose total volume is V_T. If N_o is the initial number density and N is the number density at time t, then the corresponding numbers of reactant molecules in the cell are N_oV_T and NV_T, respectively. The number density N decreases as the reactant is used up in the chemical reaction. That portion of the focused laser radiation with intensity strong enough to produce a reaction occupies a small volume in a region near the lens' focus. This reaction volume, denoted by V_R, is a fraction of the total volume and at time t contains an amount of reactant equal to NV_R. If it is assumed that all the reactant molecules in the reaction volume react with each laser pulse and the reaction volume is constant, then the reaction rate can be written as

$$\frac{d(NV_T)}{ds} = NV_R \ , \qquad (A.1)$$

where s is the number of laser pulses. This equation further assumes that the back reaction is sufficiently slow that only one term is necessary to describe the process. Solving this equation yields

$$\ln\ (N/N_o) = -\ \frac{V_R}{V_T}\ s \ . \qquad (A.2)$$

Thus, a plot of $\ln(N/N_o)$ as a function of the number of laser pulses yields a straight line whose slope is the ratio of the reaction volume to the total volume. If $\ln\ (N/N_o)$ is not a linear function of s, then the assumptions of constant reaction volume or of complete reaction are in error.

To relate the reaction volume to a threshold intensity it is

necessary to calculate the volume of an isointensity surface in a region near the focus. Although diffraction effects are important in determining this volume, ease of calculation prompted consideration of two limiting cases: focusing of paraxial rays and focusing of an ideal Gaussian beam.

Focusing of paraxial rays is based strictly on geometric considerations and the reaction volume consists of two cones joined at their apexes as indicated in Figure A.1(a). In the small angle approximation the volume is calculated to be

$$V_R \sim \frac{2\pi\, h^3\, \delta^2}{3} \quad , \tag{A.3}$$

where h is the cone height and $\delta = r/h$ is the cone angle. The f/number of the lens is related to the cone angle and can be defined as $f = 1/2\,\delta$. If the threshold intensity is defined as the total power in the laser beam divided by the area of the base of the cone, then Equation (A.4) can be rewritten in terms of the power, P, the threshold intensity, I_R, and the focal length, f. That is,

$$V_R = \frac{4}{3\sqrt{\pi}}\, f \left(\frac{P}{I_R}\right)^{3/2} . \tag{A.4}$$

The intensity at the base of the cones, I_R is related to the volume of the cones by

$$I_R = \left(\frac{4}{3\sqrt{\pi}}\right)^{2/3} P \left(\frac{f}{V_R}\right)^{2/3} . \tag{A.5}$$

The derivation of the reaction volume and threshold intensity for the ideal Gaussian beam is more involved. The beam is focused to a

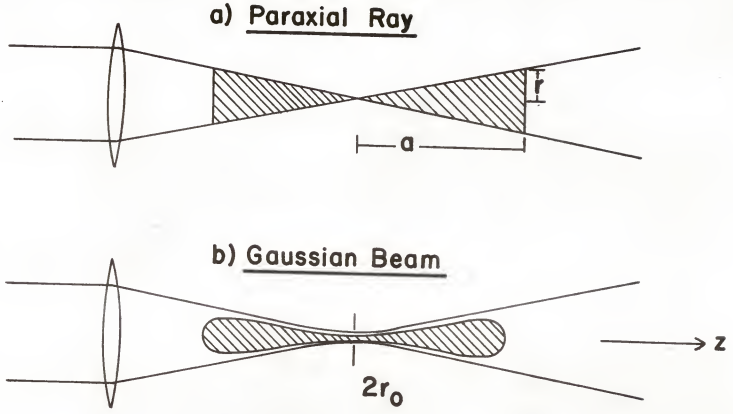

Figure A.1 Two limiting cases for the reaction volume calculation.

spot of radius

$$r_o = \frac{\lambda f}{\pi} \tag{A.6}$$

where λ is the wavelength of the radiation and f is the f/number of the lens which is again defined as $1/2\delta$. The peak intensity at the center of the focal spot is

$$I_p = \frac{P}{\pi r_o^2} \tag{A.7}$$

where, again, P is the total laser power in the beam. Using this definition for I_p, the intensity can be written as[71]

$$I(U,V) = \frac{I_p}{1+U^2} \exp\left(\frac{-V^2}{1+U^2}\right) , \tag{A.8}$$

where $U = z/2r_o f$ and $V = r/r_o$ are dimensionless axial and radial coordinates. A surface of constant intensity I_R is defined by

$$K = \frac{1}{1+U^2} \exp\left(\frac{-V^2}{1+U^2}\right) \tag{A.9}$$

where K is I_R/I_p. The maximum axial coordinate U_m of the isointensity surface occurs where the intensity drops to threshold on the beam axis; that is, V = 0 or

$$U_m = \sqrt{\frac{1}{K} - 1} . \tag{A.10}$$

The volume within the isointensity surface is

$$V_R = -4\pi r_o^3 f \int_0^{U_m} (1+U^2) \log [K(1+U^2)] \, dU. \tag{A.11}$$

Normally, $U \gg 1$ so that Equation (A.11) may be approximated by

$$V_R = -4\pi r_o^3 f \int_o^{U_m} U^2 \log KU^2 \, dU \, . \qquad (A.12)$$

Under the usual conditions for focused beams, the threshold intensity is much less than the peak intensity; that is, $K \ll 1$ so that $U_m \sim K^{-\frac{1}{2}}$. Subject to these approximations Equation (A.12) is easily evaluated and

$$V_R = \frac{8}{9\sqrt{\pi}} f \left(\frac{P}{I_R} \right)^{3/2} \, . \qquad (A.13)$$

The intensity at the surface is related to the volume by

$$I_R = \left(\frac{8}{9\sqrt{\pi}} \right)^{2/3} P \left(\frac{f}{V_R} \right)^{2/3} \, . \qquad (A.14)$$

It is interesting to note that for both the paraxial ray and Gaussian beam cases that the reaction volume increases linearly with the f/number and with the 3/2 power of the total laser power. The resulting reaction volume is schematically illustrated in Figure A.1(b). For a given experiment the reaction volume can be determined from the plot of $\ln (N/N_o)$ versus the number of pulses and the threshold intensity can be determined from Equation (A.14) if it is assumed that the reaction volume coincides with the volume within an isointensity surface.

Experimental Results

A series of experiments were performed to determine the threshold intensity using various f/numbers, laser powers, and pressures. The experimental set up is shown schematically in Figure A.2. To allow accommodation by the first lens of the two-lens system, the output of a UV preionized CO_2 TEA laser passed through a one-inch aperture. The double lens system consisted of an f/5 and an f/1.5 Ge lens with the

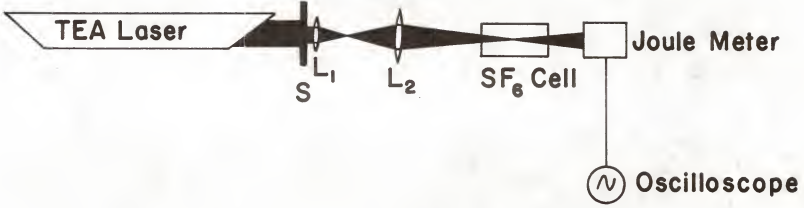

Figure A.2 Schematic diagram of the experimental set up.

longer focal length lens placed first to eliminate air breakdown between them; this arrangement facilitated variation of the effective focal length. After passing through the second lens, the beam was focused into a stainless steel cell having a volume of 51.48 cm^3 and containing SF_6 at pressures less than one torr. Since the gas cell was constructed with NaCℓ windows on each end, the emerging beam could be monitored with a pyroelectric detector whose output was displayed on an oscilloscope.

For determination of the threshold intensity the beam power in Equation (A.14) was taken to be the peak power in the pulse. A value for this power was obtained by observing the pulse shape with the pyroelectric detector and measuring the total pulse energy with a joule meter. The laser operated on a mixture of He, CO_2, and N_2 producing a pulse with an initial peak approximately 200 ns wide and a long, low power tail extending roughly 3 μs. The output of the pyroelectric detector indicated that the laser may be spontaneously mode locking. The pulse train did not exhibit the characteristics of an actively mode locked laser, but appeared as hash superimposed on a dc level. Examination of this hash indicated that it was composed of pulses that were approximately 1 to 2 nsec wide and spaced at intervals of 5 nsec. At times these pulses were 50% higher than the dc level. However, it has been shown that 1 nsec pulses are ineffective for separating isotopes;[24] therefore, the effective power was assumed to be the dc level.

The stainless steel reaction chamber was backfilled with SF_6 in natural abundance, no scavenger was used, and the concentration of

$^{32}SF_6$ measured with a Perkin-Elmer 237B grating infrared spectrometer. The spectrometer was calibrated by filling the cell to known pressures of SF_6 and noting the percent transmission at 948 cm^{-1} which is the ν_3 fundamental of $^{32}SF_6$. At the start of an experimental run the cell was filled to a pressure of 0.3 or 0.4 torr. The laser cavity was not tuned and therefore emitted on the highest gain line, the P(20) line. This line matches the ν_3 fundamental of $^{32}SF_6$ and irradiation with the laser reduces the amount of $^{32}SF_6$ in the cell as described in References 22 and 23, leaving the $^{34}SF_6$ relatively unchanged. An infrared spectrum of the cell contents centered around 948 cm^{-1} was taken after every 10 pulses starting at zero and progressing to 100 pulses. Sample spectra of the initial contents and the contents after 100 pulses are shown in Figures A.3(a) and (b). The major peak at 948 cm^{-1} is due to $^{32}SF_6$, the small shoulder at 930 cm^{-1} to $^{34}SF_6$, and the peak at 750 cm^{-1} in Figure A.3(b) is a product of the reaction tentatively identified as SF_4. Since the spectrometer had been calibrated, it was possible to relate the transmittance to the partial pressure of the remaining $^{32}SF_6$. A typical plot of $\ln (N_o/N)$ as a function of the number of laser pulses is shown in Figure A.4.

Knowing the total cell volume, V_T, and having determined the slope, $\frac{d\,\ln(N_o/N)}{ds}$ from the graph, a value for the reaction volume, V_R, can be obtained from Equation (A.2). Finally, this value for V_R and the measured value of the laser power P, can be used in Equation (A.14) to find the threshold intensity, I_R. Four experimentally determined values of I_R are listed in Table A.1 and they yield an average value of

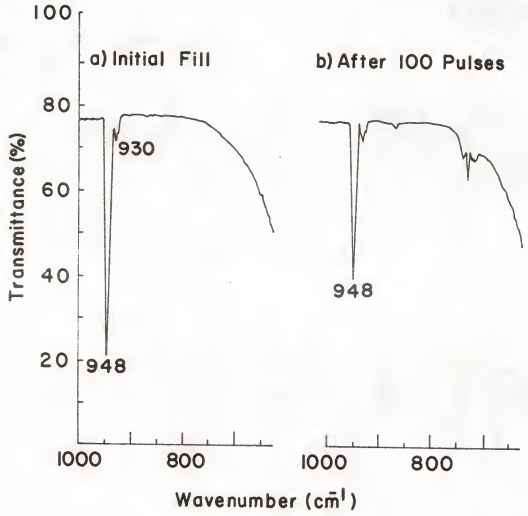

Figure A.3 Infrared spectra of SF_6. (a) Before processing (b) After 100 pulses.

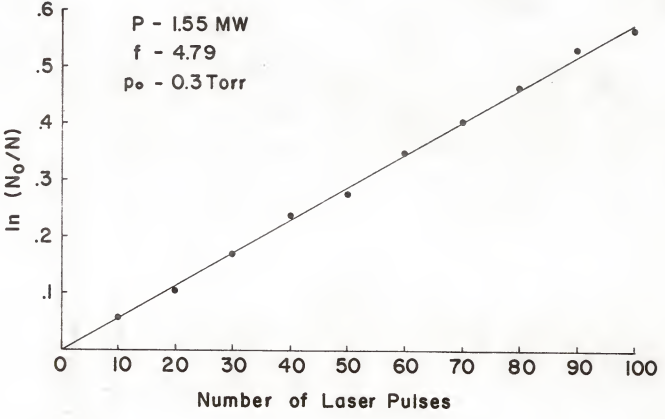

Figure A.4 Plot of $\ln (N_o/N)$ as a function of the number of laser pulses.

Table A.1

Data for four threshold intensity experiments

Run	Initial fill pressure-p_o(torr)	f/number	Laser power-P (MW)	Reaction volume-V_r (cm^3)	Threshold Intensity-I_R (MW/cm^2)
1	0.3	4.79	1.59	.322	6.07
2	0.3	4.79	1.55	.296	6.28
3	0.3	2.91	1.70	.232	5.80
4	0.4	2.91	1.72	.224	6.00

Average value $I_R = 6.04\ MW/cm^2$

6.04 ± 0.24 MW/cm^2 for the threshold intensity. This power density is some two orders of magnitude smaller than previously reported values.[18,22-24]

The results of the experimental study indicate that the linear relationship of ln (N_o/N) with the number of laser pulses predicted by Equation (A.2) is indeed observed. This justifies the assumption of constant reaction volume and supports the assumption of a sharp threshold for the laser-induced dissociation process. The dependence of the reaction volume on f/number and laser power predicted by Equation (A.13) is also in agreement with the observed results within experimental error.

The relatively large reaction volumes (0.2-0.3 cm^3) and low value of threshold intensity (6 MW/cm^2) found in this study eliminate both dynamic Stark broadening[27] and dissociative electron attachment[26] as mechanisms for laser-induced isotope separation in SF_6 since both mechanisms require higher intensity thresholds. However, this does not eliminate dissociative electron attachment as a viable mechanism for isotope separation.

The absolute value of the threshold intensity may be in error by as much as 50% due to the theoretical assumptions and the experimental error. However, this does not alter the preceding conclusions.

LIST OF REFERENCES

1. A. L. Schawlow and C. H. Townes, Phys. Rev. 112, 1940 (1958).

2. T. H. Maiman, Nature 187, 493 (1960).

3. A. Javan, W. R. Bennett, Jr., and D. R. Herriott, Phys. Rev. Lett. 6, 106 (1961).

4. J. A. Beaulieu, Appl. Phys. Lett. 16, 504 (1970).

5. Laser Focus 10(2), 6 (1974).

6. Science 191, 1162 (1976).

7. Laser Focus 11(7), 16 (1975).

8. Laser Focus 10(8), 10 (1974).

9. Laser Focus 9(12), 18 (1973).

10. C. B. Moore, Acct. Chem. Res. 6, 323 (1973).

11. A. F. Bernhardt, D. E. Duerre, J. R. Simpson, and L. L. Wood, Appl. Phys. Lett. 5, 109 (1974).

12. Laser Focus 9(11), 4 (1973).

13. U. S. Patent 3,772,519 to R. H. Levy and G. S. Janes for Jersey Nuclear-Avco Isotopes Inc.

14. S. A. Tuccio, J. W. Dubrin, O. G. Peterson, and B. B. Snavely, IFEE J. Quant. Elect. Q.E.11, 101D (1975).

15. M. Lamotte, H. J. Dewey, R. A. Keller, and J. J. Ritter, Chem. Phys. Lett. 30, 164 (1975).

16. D. D.-S. Liu, S. Dotta, and R. N. Zare, J. Amer. Chem. Soc. 97, 2557 (1975).

17. S. D. Rockwood and S. W. Rabideau, VIII Intern. Quantum Electron. Conf. (1974).

18. S. M. Freund and J. J. Ritter, Chem. Phys. Lett. 32, 255 (1975).

19. E. S. Young and C. B. Moore, Appl. Phys. Lett. 21, 109 (1972).

20. R. V. Ambartzumian, V. S. Letokhov, G. N. Makarov, and A. A. Puretskii, J.E.T.P. Lett. 17, 63 (1973).

21. R. V. Ambartzumian, V. S. Letokhov, E. V. Ryabov, and N. V. Chekalin, Zh. Eksp. Teor. Fiz. Pisma Red 20, 597 (1974).

22. R. V. Ambartzumian, Y. A. Gorokhov, V. S. Letokhov, and G. M. Markarov, Zh. Eksp. Teor. Fiz. Pisma Red 21, 375 (1975).

23. J. L. Lyman, R. J. Jensen, J. Rink, C. P. Robinson, and S. D. Rockwood, Appl. Phys. Lett. 27, 87 (1975).

24. J. L. Lyman and S. D. Rockwood, J. Appl. Phys. 47, 595 (1976).

25. H. C. Schau, III, Doctoral Dissertation, University of Florida (1975).

26. J. E. Allen, Jr., D. R. Keefer, and W. B. Person, Appl. Phys. Lett., 27, 474 (1975).

27. R. V. Ambartzumian, N. V. Chekalin, V. S. Doljikov, V. S. Letokhov, and E. A. Ryabov, Chem. Phys. Lett. 25, 15 (1974).

28. V. N. Bagratashvili, I. N. Knyazev, V. S. Letokhov, and V. V. Lobko, Optics Commun. 14, 426 (1975).

29. R. V. Ambartzumian, N. V. Chekalin, V. S. Letokhov, and E. A. Ryabov, Chem. Phys. Lett. 36, 301 (1975).

30. S. D. Rockwood, "Laser Induced Chemiluminescence of BCl_3/H_2S Mixtures" (to be published in Chem. Phys. Lett.).

31. C. L. Chen and P. J. Chantry, 28th Annual Gaseous Electronics Conference, Rolla, Missouri (1975).

32. Laser Focus 9(8), 34 (1973).

33. R. A. Keller, Physical Chemistry Seminar, University of Florida (1975).

34. G. Herzberg, Infrared and Raman Spectra of Polyatomic Molecules, New York: D. Van Nostrand Reinhold Co. (1945).

35. R. T. Lagemann and E. A. Jones, J. Chem. Phys. 19, 534 (1951).

36. J. Gaunt, Trans. Faraday Soc. 49, 1122 (1953).

37. H. Brunet and M. Perez, J. Mol. Spectrosc. 29, 472 (1969).

38. V. D. Klimov and E. A. Lobikov, Optics and Spectroscopy 30, 25 (1971).

39. J. P. Aldridge, H. Filip, H. Flicker, R. Holland, R. S. McDowell, N. G. Nereson, and K. Fox, J. Mol. Spectrosc. 58, 165 (1975).

40. Handbook of Chemistry and Physics 41st Edition, edited by C. D. Hodgman, R. C. Weast, and S. M. Selby, Cleveland: Chemical Rubber Publishing Co., 1960.

41. M. S. Foster and J. L. Beauchamp, Chem. Phys. Lett. 31, 482 (1975).

42. R. N. Compton, L. G. Christophorou, G. S. Hurst, and P. W. Reinhardt, J. Chem. Phys. 45, 4634 (1966).

43. L. G. Christophorou, D. L. McCorkle, and J. G. Carter, J. Chem. Phys. 54, 253 (1971).

44. F. C. Fehsenfeld, J. Chem. Phys. 53, 2000 (1970).

45. W. M. Hickam and R. E. Fox, J. Chem. Phys. 25, 642 (1956).

46. J. A. D. Stockdale, R. N. Compton, and H. C. Schweinler, J. Chem. Phys. 53, 1502 (1970).

47. A. Herzenberg, Abstracts of the VIIth International Conference on the Physics of Electronic and Atomic Collisions, Amsterdam: North-Holland Co. (1971).

48. P. W. Harland and J. C. J. Thynne, J. Phys. Chem. 75, 3517 (1971).

49. J. M. S. Henis and C. A. Mabie, J. Chem. Phys. 53, 2999 (1970).

50. R. W. Odum, D. L. Smith, and J. H. Futrell, Chem. Phys. Lett. 24, 227 (1974).

51. C. E. Klots, J. Chem. Phys. 46, 1197 (1967).

52. C. Lifshitz, A. MacKenzie Peers, R. Grajower, and M. Weiss, J. Chem. Phys. 53, 4605 (1970).

53. D. Spence and G. J. Shulz, J. Chem. Phys. 58, 1800 (1973).

54. C. L. Chen and P. J. Chantry, Bull. Am. Phys. Soc. 15, 418 (1970).

55. F. A. Gianturco, Chem. Phys. Lett. 17, 127 (1972).

56. C. E. Klots, Chem. Phys. Lett. 38, 61 (1976).

57. J. Kay and F. M. Page, Trans. Faraday Soc. 60, 1042 (1964).

58. F. C. Fehsenfeld, J. Chem. Phys. 54, 438 (1971).

59. P. R. Hammond, J. Chem. Phys. 55, 3468 (1971).

60. C. Lifshitz, B. M. Hughes, and T. O. Tiernan, Chem. Phys. 7, 469 (1970).

61. C. Lifshitz, T. O. Tiernan, and B. M. Hughes, J. Chem. Phys. 59, 3182 (1973).

62. R. N. Compton and C. D. Cooper, J. Chem. Phys. 59, 4140 (1973).

63. T. L. Cottrell, The Strength of Chemical Bonds, London: Butterworths Publications Ltd. (1958).

64. C. B. Leffert, S. Y. Tang, E. W. Rothe, and T. C. Cheng, J. Chem. Phys. 61, 4929 (1974).

65. G. Herzberg, Spectra of Diatomic Molecules, New York: D. Van Nostrand Reinhold Co. (1950).

66. S. Abramowitz and I. W. Levin, J. Chem. Phys. 44, 3353 (1966).

67. R. J. Zollweg, J. Chem. Phys. 50, 4251 (1969).

68. A. W. Nowak and J. L. Lyman, J. Quant. Spectrosc. Radiat. Transfer 15, 945 (1975).

69. W. Becher and J. Massonne, ETZ: Electrotechnische Zeitschrift 91A, 605 (1970).

70. G. Gioumousis and D. P. Stevenson, J. Chem. Phys. 29, 294 (1958).

71. D. J. Innes and A. L. Bloom, Spectra-Physics Laser Tech. Bull. No. 5 (1966).

BIOGRAPHICAL SKETCH

John Edward Allen, Jr. was born April 12, 1945 in Lakeland, Florida. In January, 1963 he was graduated from Lanphier High School in Springfield, Illinois. In April, 1967, he received the degree of Bachelor of Science in Physics and in August, 1970, the degree of Master of Science in Physics both from the University of Florida. He is a member of the American Scientific Affiliation, Sigma Pi Sigma, and Tau Beta Pi.

He is the father of two children, John Edward III and Michael Lee.

I certify that I have read this study and that in my opinion it conforms to acceptable standards of scholarly presentation and is fully adequate, in scope and quality, as a dissertation for the degree of Doctor of Philosophy.

Dennis R. Keefer, Chairman
Associate Professor of Engineering Sciences

I certify that I have read this study and that in my opinion it conforms to acceptable standards of scholarly presentation and is fully adequate, in scope and quality, as a dissertation for the degree of Doctor of Philosophy.

Mark H. Clarkson
Professor of Engineering Sciences

I certify that I have read this study and that in my opinion it conforms to acceptable standards of scholarly presentation and is fully adequate, in scope and quality, as a dissertation for the degree of Doctor of Philosophy.

Bernard M. Leadon
Professor of Engineering Sciences

I certify that I have read this study and that in my opinion it conforms to acceptable standards of scholarly presentation and is fully adequate, in scope and quality, as a dissertation for the degree of Doctor of Philosophy.

Earle E. Muschlitz
Professor of Chemistry

I certify that I have read this study and that in my opinion it conforms to acceptable standards of scholarly presentation and is fully adequate, in scope and quality, as a dissertation for the degree of Doctor of Philosophy.

Willis B. Person
Professor of Chemistry

I certify that I have read this study and that in my opinion it conforms to acceptable standards of scholarly presentation and is fully adequate, in scope and quality, as a dissertation for the degree of Doctor of Philosophy.

Thomas L. Bailey
Professor of Physics

I certify that I have read this study and that in my opinion it conforms to acceptable standards of scholarly presentation and is fully adequate, in scope and quality, as a dissertation for the degree of Doctor of Philosophy.

Lennart R. Peterson
Associate Professor of Physics

This dissertation was submitted to the Dean of the College of Engineering and to the Graduate Council, and was accepted as a partial fulfillment of the requirements for the degree of Doctor of Philosophy.

June, 1976

Dean, College of Engineering

Dean, Graduate School